Effects of Boundaries On Rayleigh-Bénard Convection

Thesis by

Yih-Yuh Chen

In Partial Fulfillment of the Requirements

for the Degree of

Doctor of Philosophy

California Institute of Technology

Pasadena, California

1991

(Defended May 29, 1991)

(Thesis Advisor: M.C. Cross)

Acknowledgment

Writing up this acknowledgment is difficult for me not only because the gratitude in my heart just cannot be expressed in simple words, but also because this means goodbye to many of the most wonderful people who have helped make this work possible. My deepest thanks go first to my advisor Prof. M. C. Cross, who has always been there to give me guidance, to encourage me, to support me, and to give me complete freedom to explore all the beautiful things in physics that have fascinated me so much. His understanding and patience also made difficult moments of my life easier. His modesty and physics insight are testimonies to a truly great scientist!

Profs. P. -H. Tsao and J. Chen of National Taiwan University have given me encouragement and invaluable advice through every step of my academic life. They know a simple thanks here gives only a hint of how I feel about them. Profs. P. -K. Tseng and W. -H. Huang also proved a teacher's care about a student really makes a difference and helps him stand up.

My friends K. -S. Huang, T. -M. Hong, J. -Y. Lee, Z. -Y. Su and H. W. Chang taught me interesting things in other fields and showed me different aspects of science. Without their constant good words and helpful information the road would have been much bumpier and less exciting. My feedback to M. S. Bourzutschky and E. Kuo can only be described as minimal when compared to what they have offered me in each discussion! My brother E. T. has been my biology teacher who

showed me physics can be applied to life sciences to produce results that were never correctly predicted by me, and I thank him for opening my eyes.

Discussions with Profs. H. B. Keller and N. -C. Yeh clarified and helped me understand some subtle points of my research, and I am grateful for their enthusiasm and generosity with their time.

Our secretary Pat Stevens has been so nice in helping me with my papers and thesis that I almost volunteered to be her errand boy in return for her kindness!

Last, but certainly not least, I thank my parents for having full and blind faith in me. They know nothing about physics, and have no idea what doing research is like, yet they have given me full-hearted support in the career I have chosen. Their devotion and determination to give me the best environment has made my journey in physics all the more enjoyable and rewarding. And, with love, this work is dedicated to them, the best parents in the world!

Abstract

The effects of boundary conditions on the linear stability of finite cell pure fluid Rayleigh-Bénard convection are investigated *via* a variational formalism and a perturbative approach. Some general properties of the critical Rayleigh number, R_C, with respect to change of boundary conditions or system size are derived. I argue that R_C differs from its infinite cell limit by an amount that is inversely proportional to the square of the system size, and that the fluid variables must become vanishingly small near the sidewall when compared to their bulk values, thus generalizing the known results derivable from the amplitude equation approach for a two-dimensional problem. It is also shown that the reaction-diffusion models of spatial pattern forming systems in developmental biology can be thought of as a special case of the convection problem. The similarity and major difference between the two systems are discussed. I also show that, as far as the onset stability is concerned, one can replace the sidewall of a convection cell by a mathematically simpler homogeneous boundary condition while still retaining the basic physics involved.

Table of Contents

List Of Figures

Chapter 1: Introduction

§1.1 Organization Of This Work:

Rayleigh-Bénard convection has been an intensively studied problem in recent years for several reasons: (1) From the experimental point of view a layer of fluid uniformly heated from below is simple to study, and the experimental setup can be well controlled. (2) The pattern formation and dynamics of this system are very rich, and bear several features common to other reaction-diffusion systems that are of interest to people working in different fields. (3) The governing equations for the system are simple and admit reasonably general and powerful techniques for theoretical treatment.

Although it is true that a considerable amount of analytic results in the weakly nonlinear regime of the convection problem have been derived, relatively little about the *linear* problem is known thoroughly when the effects of the boundaries are explicitly taken into account. A major focus of the present work, therefore, is devoted to this problem. This is of great interest because the finiteness of the convection cell can significantly increase the complexity of the dynamics and put constraints on the formation of patterns inside the cell. For example, the reflections of a traveling wave can interact with the original wave in a very complicated manner if the sidewall is present. Also, the convective rolls might have to adjust themselves in such a way that they can be accommodated by the geometry of the convection cell and the imposed boundary conditions are satisfied. This certainly

will constrain the allowed patterns in a cell. Because of the obvious intractability of the full problem by a rigorous approach at this moment, not to mention that other complications, such as rotation or the presence of impurity which could cause even richer phenomena, I have decided to concentrate on the simplest case in which only the convective instability of finite cell pure fluid is considered. I believe this is the first step toward a better understanding of how the sidewall influences the bulk fluid. A somewhat more analytical approach is taken in this work in the hope that it might shed some light on why or when other more phenomenological approaches are expected to work. In addition, this can also serve as an independent verification of predictions made by other approaches whenever comparison is possible.

The presentation of the results of this study is organized in the following order: In Chapter 2, I show how the linear stability problem can be formulated in terms of variational principles. This is desirable because from the theoretical point of view it helps us exclude some possible pathological behavior in other systems that do not admit such formulation. For example, the eigenvalues of this system are real and can never coalesce to form a complex conjugate pair. This, then, implies the eigenvalues will change in a well-defined way when we vary adjustable parameters of the system, a result that is essential to my approach and used extensively in this work. Having shown the possibility of expressing both the growth rate in time and the critical Rayleigh number in terms of variational principles, I then go on to show that this formalism easily predicts monotonic

dependence of system stability on properties of the sidewall, such as its thickness and thermal conductivity. Several other monotonicity theorems are also presented. A simplified "surrogate" homogeneous boundary condition modeling the effects of the sidewall that has been commonly used in this field, and which seems capable of capturing the underlying physics, is then introduced. Its corresponding variational formulation is briefly discussed. This paves the way to Chapter 3, which is devoted to investigating, in detail, the properties associated with this "surrogate system."

I develop in Chapter 3 a perturbation theory and combine it with results obtained in Chapter 2 to derive, among other things, the effects of cell size on stability and the size scaling behavior of the critical Rayleigh number of the surrogate system. I give an argument that makes it apparent that the spatial pattern-forming mechanism characteristic of the reaction-diffusion models of developmental biology can be viewed as a special case of the convection problem. The difference and similarity of the two systems are pointed out and discussed. I close the chapter by showing that the surrogate system indeed simulates the real system in a mathematically well-defined way, thus justifying the original simplification.

In Chapter 4, a very simple-minded picture of the behavior of a convective roll near the sidewall is proposed as a physical argument for the orthogonality of the roll to the sidewall. Though completely nonlinear in principle, the argument I propose is linear in nature because *the fluid equations become linear near the sidewall when realistic boundary conditions are imposed.*

Chapter 5 concludes my investigation and points out other problems awaiting further research. I also include Appendix A to illustrate the ideas and verify the predictions of the main text. Appendix B supplements the text by providing a brief discussion of the feasibility of separation of variables for the problem at hand.

In this first chapter, however, I will give a brief review of the history and some of the simple characteristic phenomena observed in experiments, derive the governing equations to be studied in later chapters, and explain the observed features in terms of simple physical arguments.

§1.2 Brief History:

In 1900, Bénard performed the first quantitative experiments[1] which later initiated much theoretical and experimental work on the convective instability of a layer of fluid heated from below which is now known as "Rayleigh-Bénard convection," though according to Drazin and Reid[2] the first one to describe this convective instability seems to be J. Thomson.[3] In 1916, Lord Rayleigh published the first theoretical treatment of this problem under the mathematically simpler assumption of free-slip boundary condition.[4] Numerical solutions generalizing his theory to cover cases with realistic boundary conditions were subsequently developed by Jeffreys[5] and Low.[6] In 1940, Pellew and Southwell[7] succeeded in formulating the linear stability of a laterally unbounded system in terms of a variational principle, which was later generalized by Sorokin[8] to a finite system with either a perfectly insulating or a perfectly conducting sidewall. The study of nonlinear pure fluid

convection caught the scientific community by surprise when in 1963, Lorenz discovered a strange attractor in a simple three-mode Galerkin truncation model of the atmospheric convective motion.[9] Later, Segel[10] and Newell and Whitehead[11] developed the amplitude equation approach that is capable of describing many weakly nonlinear phenomena in one-dimensional systems. Their method is now widely used in many other fields to treat different problems. Meanwhile, convection problems with other complications had also been studied intensively. These include the rotating convection problem that is directly related to solar dynamics and geophysical flows, binary fluid convection that becomes unstable through Hopf bifurcation, and convection in porus media, just to name a few. It is interesting to note that the cellular pattern originally observed by Bénard was later concluded to be caused not by buoyant instability, but by surface tension at the air-liquid interface.[12,13]

§1.3 Governing Equations:

Consider a layer of pure fluid placed in between two horizontal plates whose temperatures are fixed in such a way that the bottom is warmer than the top. (See Fig. 1.1.) Denote this convection cell by Ω. In most experiments the thickness d of the fluid layer is several millimeters and the temperature difference ΔT across the layer is several Kelvin. The system is stable and remains in a quiescent, structureless, purely thermal conducting state unless ΔT exceeds some critical value. When instability sets in because of the increased temperature gradient, cellular pattern

of convective rolls with a characteristic wavelength$\approx d$ forms spontaneously.

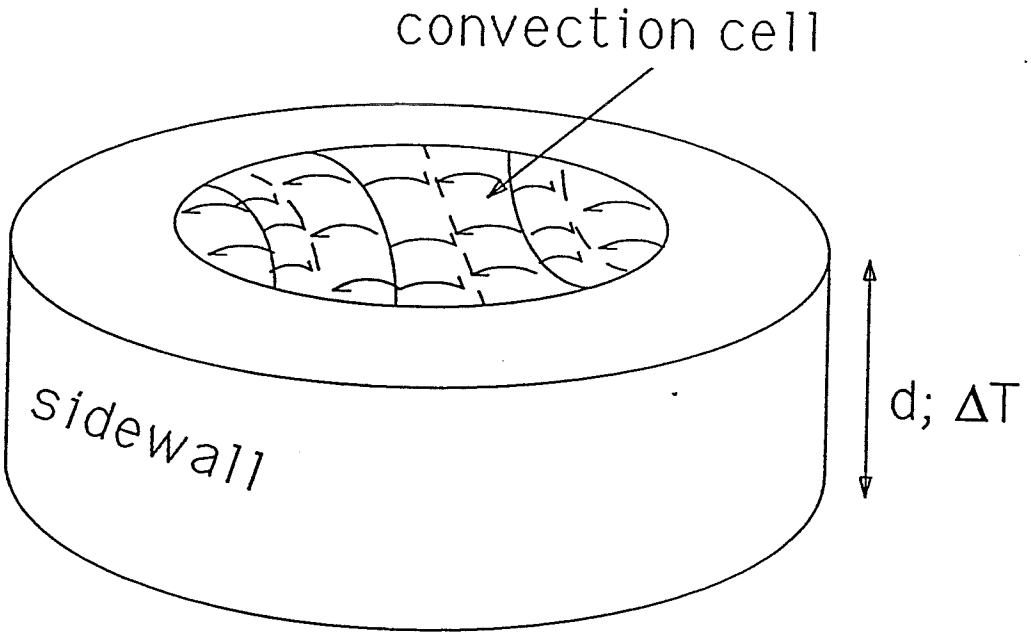

Figure 1.1: Schematic drawing of the experimental setup for Rayleigh-Benard convection.

If ΔT doesn't exceed its critical value by too much, the system will settle down to a time-independent state with the described roll structure. It is commonly observed that the convective rolls have the tendency of aligning themselves normal to the sidewall of the convection cell.[14–18] Complicated dynamics sets in if ΔT is increased further.

The governing equations describing the time evolution of fluid velocity $\vec{v}$, temperature T, pressure P and density ρ are the Navier-Stokes equation, heat transport

equation, and mass conservation law:

$$\frac{\partial \vec{v}}{\partial t} + (\vec{v} \cdot \nabla)\vec{v} = \frac{-1}{\rho}\nabla P - g\hat{e}_z + \nu\nabla^2\vec{v} \ , \tag{1}$$

$$\frac{\partial T}{\partial t} + (\vec{v} \cdot \nabla)T = \kappa\nabla^2 T \ , \tag{2}$$

$$\frac{\partial \rho}{\partial t} + \nabla \cdot (\rho\vec{v}) = 0 \ , \tag{3}$$

where ν and κ are the kinematic viscosity and thermal diffusivity of the fluid, respectively. Here g is the gravitational acceleration which acts in the opposite direction to the vertical normal $\hat{e}_z$. The time-independent conduction profile (subscripted by c) is given by

$$\begin{aligned} T_c &= T_1 - \frac{z}{d}\Delta T \ , \\ \nabla P_c &+ \rho_c g\hat{e}_z = 0 \ , \end{aligned} \tag{4}$$

with $T_1 \equiv$ temperature of the bottom plate, and ρ_c being some known thermodynamic function of T_c (equation of state). For many experiments it suffices to assume $\rho = \rho_1(1 - \gamma(T - T_1))$, where ρ_1 is the fluid density at temperature T_1 and γ is the (constant) thermal expansion coefficient, though one must bear in mind the peculiar property of water at 4^oC. With this assumption we can rewrite Eqns. (1) through (3) in terms of deviations from the conduction profile:

$$\frac{\partial \vec{v}}{\partial t} + (\vec{v} \cdot \nabla)\vec{v} = \frac{-1}{\rho}\nabla\delta P - \frac{\rho_1}{\rho}g\gamma\delta T\hat{e}_z + \nu\nabla^2\vec{v} \ , \tag{5}$$

$$\frac{\partial \delta T}{\partial t} + (\vec{v} \cdot \nabla)\delta T = \kappa\nabla^2\delta T + \frac{\Delta T}{d}v_z \ , \tag{6}$$

$$\nabla \cdot \vec{v} = \frac{\rho_1}{\rho}\gamma(\kappa\nabla^2\delta T) \ , \tag{7}$$

where the last equation is obtained by comparing Eqns. (3) and (6). When the two terms of the R.H.S. of Eqn. (6) are of the same order of magnitude, as is the case if we consider the linear stability of the onset configuration, Eqn. (7) gives

$$|\nabla \cdot \vec{v}| = \gamma \Delta T \frac{\rho_1}{\rho} \mathcal{O}(\frac{v_z}{d}) \ .$$

For water at room temperature $\gamma = 6.427 \times 10^{-5} {}^{o}\mathrm{C}^{-1}$,[19] and we see that $\nabla \cdot \vec{v}$ is practically zero in order of magnitude. This suggests the "Oberbeck-Boussinesq approximation," which assumes that (1) all the coefficients in Eqns. (5) and (6) can be treated as constants, and (2) that Eqn. (7) can be approximated by the incompressibility condition $\nabla \cdot \vec{v} = 0$. This argument also suggests the possibility of expanding the solution in terms of the small parameter $\gamma \Delta T$, if non-Boussinesq effects are not negligible. A more rigorous and general approach along this line already exists in the literature.[20-22] In the following, I will simply adopt this approximation without further discussion.

Eqns. (5) and (6) and the incompressibility condition can be cast into a dimensionless form if we scale length, time and temperature by d, d^2/κ, and $\kappa\nu/\gamma g d^3$, respectively:

$$\frac{\partial \vec{u}}{\partial t} + (\vec{u} \cdot \nabla)\vec{u} = \sigma \nabla^2 \vec{u} + \sigma \theta \hat{e}_z - \nabla p \tag{8}$$

$$\frac{\partial \theta}{\partial t} + (\vec{u} \cdot \nabla)\theta = \nabla^2 \theta + R u_z \quad (u_z \equiv \vec{u} \cdot \hat{e}_z) \tag{9}$$

$$\nabla \cdot \vec{u} = 0 \ . \tag{10}$$

Here $\vec{u}$ and θ are the dimensionless deviations of velocity and temperature from

the pure conduction profile, respectively, whereas $\sigma \equiv \nu/\kappa$ and $R \equiv \gamma g d^3 \Delta T/(\kappa\nu)$ are respectively called the Prandtl number and the Rayleigh number.

The fluid also interacts with the sidewall Ω_w, whose dimensionless thermal conductivity is κ_w through heat exchange across their interface S. Denote the ratio of heat capacity per unit volume of the sidewall and the fluid by r, then the dimensionless temperature θ_w in the sidewall is assumed to satisfy

$$\frac{\partial \theta_w}{\partial t} = \kappa_w \nabla^2 \theta_w \quad \text{in } \Omega_w \ , \tag{11}$$

$$\theta_w = \theta \ , \quad \frac{\partial \theta}{\partial n} = r\kappa_w \frac{\partial \theta_w}{\partial n} \quad \text{on } S \ , \tag{12}$$

$$\frac{\partial \theta}{\partial n} = 0 \quad \text{on } S_2 \ , \tag{13}$$

where S_2 is the outer surface to the sidewall, and $\hat{n}$ is the outward normal to a surface. We also assume θ_w=0 at z=0,1. The viscous boundary conditions on $\partial\Omega$ are taken as

$$u_n \equiv \vec{u} \cdot \hat{n} = 0 \ , \tag{14}$$

$$\frac{\partial \vec{u}_\parallel}{\partial n} + \alpha \vec{u}_\parallel = 0 \ , \tag{15}$$

where $\vec{u}_\parallel$ and $\frac{\partial \vec{u}_\parallel}{\partial n}$ are the shorthand notations for the projection of $\vec{u}$ and $\frac{\partial \vec{u}}{\partial n}$ onto the boundary $\partial\Omega$, respectively, and α is a conveniently introduced nonnegative constant that can differ on the two horizontal plates and the sidewall. (The physically admissible no-slip condition corresponds to taking $\alpha = \infty$.)

§1.4 The Underlying Physics:

To understand physically why a minimum temperature difference ΔT, or equivalently R, is required to create convective instability, we shall consider the linear stability of the conduction profile. Then

$$\begin{aligned}
&\int_\Omega \vec{u}\cdot \text{Eqn.}(8) + \frac{\sigma}{R}\theta \cdot \text{Eqn.}(9) + \int_{\Omega_w} \frac{r\sigma}{R}\theta_w \cdot \text{Eqn.}(11) \\
&= \frac{1}{2}\frac{d}{dt}\left(\int_\Omega |\vec{u}|^2 + \int_\Omega \frac{\sigma}{R}\theta^2 + \int_{\Omega_w} \frac{r\sigma}{R}\theta_w^2\right) \\
&= \sigma\Bigg\{-\left(\int_\Omega |\nabla\vec{u}|^2 + \int_{\partial\Omega} \alpha|\vec{u}|^2 + \int_\Omega \frac{1}{R}|\nabla\theta|^2 + \int_{\Omega_w} \frac{r\kappa_w}{R}|\nabla\theta_w|^2\right) \\
&\qquad + 2\int_\Omega u_z\theta\Bigg\}
\end{aligned} \tag{16}$$

after integration by parts, where we have also made use of Eqns. (10) and (12) through (15). Notice that in order for the system to be stable, R must be controlled so that $\frac{d(\cdots)}{dt} < 0$ for all infinitesimal disturbances. Therefore, stability corresponds to $\{\cdots\} < 0$ on R.H.S. of Eqn. (16). Rewriting this stability criterion, we have

$$\frac{2\int_\Omega u_z\theta}{\int_\Omega |\nabla\vec{u}|^2 + \int_{\partial\Omega} \alpha|\vec{u}|^2 + \int_\Omega \frac{1}{R}|\nabla\theta|^2 + \int_{\Omega_w} \frac{r\kappa_w}{R}|\nabla\theta_w|^2} < 1\,. \tag{17}$$

In view of Eqn. (8), we see that the numerator of Eqn. (17) is twice the power supplied by the buoyancy, and the terms involving $\vec{u}$ that appear in the denominator are simply the power dissipation due to viscosity. The terms involving θ represent thermal dissipation. Hence, the stability criterion corresponds nicely to our intuition that instability occurs when the buoyancy wins over dissipation. In particular, we note that at marginal stability, Eqns. (8), (9) and (11) imply the buoyancy driven power gain, the viscous dissipation and the thermal dissipation

are all equal, and we recover Chandrasekhar's thermodynamic criterion for the onset Rayleigh number.[23]

Because the disturbances are arbitrary, we can absorb $\sqrt{1/R}$ into θ and θ_w and yield

$$\frac{2\int_\Omega u_z\theta}{\int_\Omega |\nabla\vec{u}|^2 + \int_{\partial\Omega}\alpha|\vec{u}|^2 + \int_\Omega |\nabla\theta|^2 + \int_{\Omega_w} r\kappa_w|\nabla\theta_w|^2} < \frac{1}{\sqrt{R}} \,. \tag{18}$$

The L.H.S. of Eqn. (18) apparently has a maximum that will be denoted by $1/\sqrt{R_C}$, and we immediately see that the system is stable if and only if R is less than R_C. This shows why a certain critical R_C must be exceeded in order for convective instability to set in.

To understand why a particular wavenumber is selected at the onset of instability, one can work with the stability criterion Eqn. (18). But here we give a different, yet more direct approach. Let's consider a two-dimensional convection problem for illustration. Suppose the disturbances have a very large wavenumber q. Then Eqn. (10) implies that u_x is q^{-1} smaller than u_z in order of magnitude, and Eqns. (8) and (9) reduce to

$$\frac{\partial u_z}{\partial t} \approx \sigma\frac{\partial^2 u_z}{\partial x^2} \quad , \quad \frac{\partial\theta}{\partial t} \approx \frac{\partial^2\theta}{\partial x^2} \,. \tag{19}$$

This means, basically, there are two modes: A vertical viscous mode with a decay constant σq^2, and a horizontal thermal diffusive mode with a decay constant q^2. (Fig. 1.2) Similarly, for $q \approx 0$ we deduce that $u_z \ll u_x$ and

$$\frac{\partial u_x}{\partial t} \approx \sigma\frac{\partial^2 u_x}{\partial z^2} \quad , \quad \frac{\partial\theta}{\partial t} \approx \frac{\partial^2\theta}{\partial z^2} \,, \tag{20}$$

from which one sees there is a horizontal viscous mode with a decay constant at least $\sigma\pi^2$, and a vertical thermal diffusive mode with a decay constant at least π^2. (Fig. 1.2) In other words, both large q and small q modes are stable against perturbations, and so the system must pick some intermediate q if it becomes unstable.

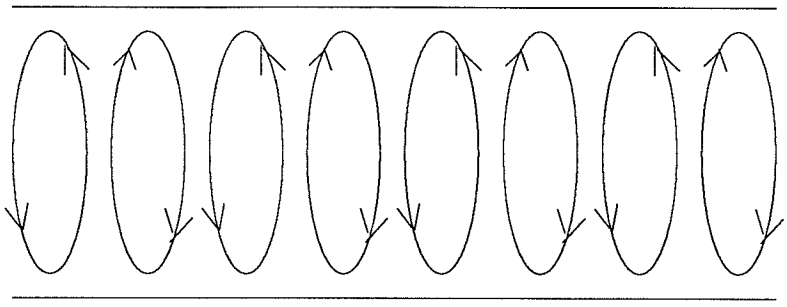

(a)

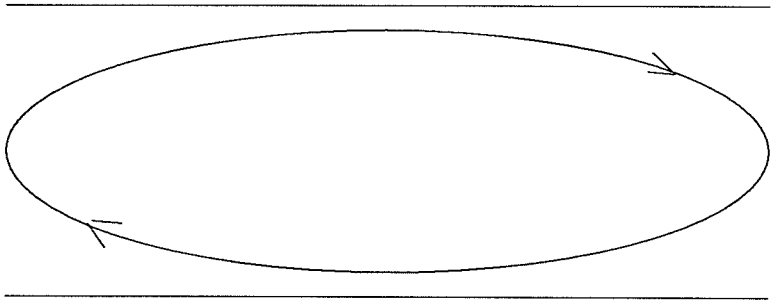

(b)

Figure 1.2: (a) Large wave number configuration is dissipated via strong vertical motion and horizontal thermal diffusion. (b) Thermal diffusion is mainly along the vertical direction, whereas viscous dissipation is due to horizontal motion when the wave number is very small.

Chapter 2: Variational Formulation Of Linear Stability Analysis

The linear stability of finite cell pure fluid convection can be formulated in terms of variational principles even when the sidewall is explicitly taken into account. This generalizes the results obtained by previous workers.[7,8] In this chapter, I will describe these variational principles and derive some monotonicity theorems directly from them. A system with a mathematically simpler thermal boundary condition is introduced together with its corresponding variational properties. Its relation to the real physical system will be relegated to the next chapter.

§2.1 Variational Principles:

It turns out that the natural (and most commonly adopted) scaling we used in Chapter 1 to render the governing equations dimensionless is not particularly convenient from the theoretical point of view when we try to formulate the linear stability problem of a convection cell in the framework of variational principles. In order to make the presentation less complicated I will adopt a slightly different scaling. If we rescale $\theta \to \sqrt{R/\sigma}\theta$ and $\theta_w \to \sqrt{R/\sigma}\theta_w$, then the linearized version

of Eqns. (1.8)*, (1.9) and (1.11) can be expressed concisely as

$$\begin{aligned}\frac{\partial \Psi}{\partial t} &= \mathcal{L}\Psi \\ &\equiv \left\{ \begin{pmatrix} \sigma & 0 & 0 & 0 & 0 \\ 0 & \sigma & 0 & 0 & 0 \\ 0 & 0 & \sigma & 0 & 0 \\ 0 & 0 & 0 & 1 & 0 \\ 0 & 0 & 0 & 0 & \kappa_w \end{pmatrix} \nabla^2 + \begin{pmatrix} 0 & 0 & 0 & 0 & 0 \\ 0 & 0 & 0 & 0 & 0 \\ 0 & 0 & 0 & \sqrt{\sigma R} & 0 \\ 0 & 0 & \sqrt{\sigma R} & 0 & 0 \\ 0 & 0 & 0 & 0 & 0 \end{pmatrix} \right\} \Psi - \begin{pmatrix} \nabla p \\ 0 \\ 0 \end{pmatrix} \\ &\equiv \left\{ \hat{D}' \nabla^2 + \sqrt{\sigma R} \hat{A} \right\} \Psi - \begin{pmatrix} \nabla p \\ 0 \\ 0 \end{pmatrix} \ , \end{aligned} \tag{1}$$

where $\hat{D}'$ and $\hat{A}$ are 5×5 matrices defined in an obvious way, and

$$\Psi \equiv \begin{pmatrix} \vec{u} \\ \theta \\ \theta_w \end{pmatrix} \equiv \begin{pmatrix} \psi \\ \theta_w \end{pmatrix} \ . \tag{2}$$

After integration by parts and using Eqns. (1.10) and (1.12) through (1.15), it is easy to show that the operator $\mathcal{L}$ is self-adjoint, provided we define the inner product between Ψ' and Ψ by

$$< \Psi' | \Psi > \equiv \int_{\Omega} \psi'^{\dagger} \cdot \psi + \int_{\Omega_w} r \theta_w'^{*} \cdot \theta_w \ , \tag{3}$$

where "†" stands for the complex conjugate of the transposition of a vector. Thus, the eigenvalues λ of $\mathcal{L}$ are real, and to determine the onset Rayleigh number one

---

* An equation referred to in other chapters will be preceded by its chapter number then followed by its equation number. Equations in the same chapter will be referred to by their equation numbers alone. This convention will also be adopted for the numbering of theorems and lemmas.

can simply set $\frac{\partial \Psi}{\partial t}$=0. Associated with $\mathcal{L}$ is a variational principle which apparently has the following form:

Variational Principle I.

The growth rate λ of Eqn. (1) is a stationary value of the following variational functional $I[\Psi]$, whose trial function Ψ must satisfy Eqns. (1.10), (1.12), (1.14) and $\theta = \theta_w = 0$ at $z = 0$ and 1:

$$I[\Psi] \equiv \frac{-\left(\int_\Omega \sigma|\nabla\vec{u}|^2 + \int_{\partial\Omega} \sigma\alpha|\vec{u}|^2 + \int_\Omega |\nabla\theta|^2 + \int_{\Omega_w} r\kappa_w|\nabla\theta_w|^2\right) + 2\sqrt{\sigma R}\int_\Omega u_z\theta}{\int_\Omega |\vec{u}|^2 + \int_\Omega \theta^2 + \int_{\Omega_w} r\theta_w^2} . \quad (4)$$

It is straightforward to verify that the function Ψ that renders $I[\Psi]$ stationary is precisely the eigenfunction of $\mathcal{L}$ associated with λ which satisfies the correct boundary conditions Eqns. (1.13) and (1.15).

Before discussing properties associated with this variational principle we need to derive two lemmas that will be used later.

Lemma 1.

For any given function g defined in a domain Ω whose topology is not necessarily that of a ball, the following inequality holds:

$$\frac{\int_{\partial\Omega} g^2}{\int_\Omega g^2} \leq c_1\sqrt{\frac{\int_\Omega |\nabla g|^2}{\int_\Omega g^2}} + c_2 \quad (5)$$

for some positive constants c_1 and c_2 that only depend on the geometry of Ω but not g.

Proof:

We can find a tubular neighborhood N near $\partial\Omega$ that is completely inside Ω, and cover all of N by a finite number of patches with polar-like coordinates (ξ_j,η_j) $(0\leq \xi_j \leq 1)$ such that: (1) $(\xi_j=0,\eta_j)$ represents the "inner" boundary $\partial N\backslash\partial\Omega$ of N, (2) ξ_j is the normalized arc length along any ξ_j-curve, (3) $(\xi_j = 1,\eta_j)$ describes the boundary $\partial\Omega$,and (4) the angle γ between the basis vector $\frac{\partial}{\partial\xi_j}$ and the surface normal $\hat{n}$ on $\partial\Omega$ is always less than and bounded away from $\frac{\pi}{2}$, as shown in Fig. 2.1. Notice ξ_j is like the radius, while η_j is like the angular coordinate. In order to simplify the notation, we'll also drop the subscript j in the following derivation.

Let f$\equiv \xi^s$ for some s$\geq$1, and let J be the Jacobian, then

$$\begin{aligned}\int_{\partial\Omega} g^2 &= \int_{\xi=1} g^2 \frac{J}{\cos\gamma} d\eta \leq \frac{1}{c}\int_{\xi=1} g^2 J d\eta \\ &= \frac{1}{c}\left(\int_{\xi=1} g^2 J f d\eta - \int_{\xi=0} g^2 J f d\eta\right) \\ &= \frac{1}{c}\int_0^1 d\xi \frac{d}{d\xi}\int_\xi g^2 J f d\eta \\ &= \frac{1}{c}\int_0^1 d\xi\left(\int_\xi 2g\frac{\partial g}{\partial\xi} J f d\eta + \int_\xi g^2 \frac{\partial(Jf)}{\partial\xi} d\eta\right)\end{aligned}$$

for some constant c.

But,

$$\left|\int_0^1 d\xi \int_\xi g\frac{\partial g}{\partial\xi} J f d\eta\right| = \left|\int_{iN} g\frac{\partial g}{\partial\xi} f\right| \leq \int_N |g|\cdot|\frac{\partial g}{\partial\xi}|$$

$$\leq \sqrt{\int_N g^2 \cdot \int_N |\frac{\partial g}{\partial\xi}|^2} \leq l\sqrt{\int_N g^2 \cdot \int_N |\nabla g|^2} \leq l\sqrt{\int_\Omega g^2 \cdot \int_\Omega |\nabla g|^2}\ ,$$

where l is the maximal arc length of ξ curves from the inner surface of N to $\partial\Omega$,

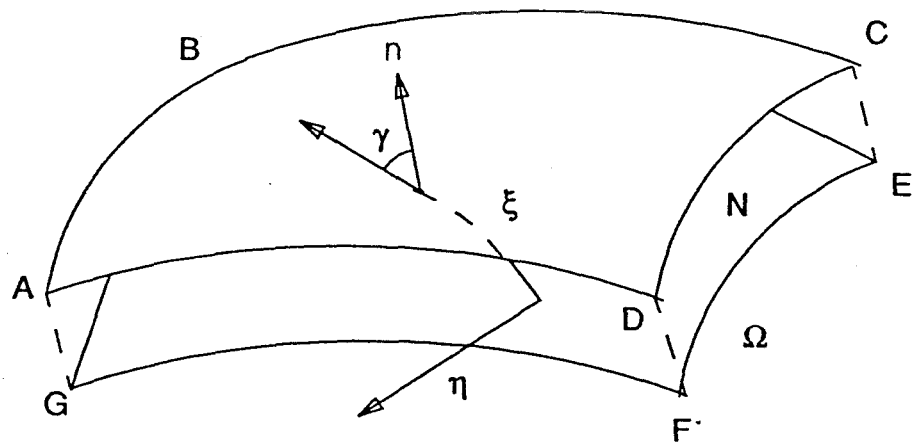

Figure 2.1: Local coordinates in a tubular neighborhood N
of the exterior surface ABCD to a domain Ω.

and we had used Cauchy-Schwarz inequality and the fact that the directional derivative of θ is never larger than its gradient.

Also,

$$\left| \int_0^1 d\xi \int_\xi g^2 \frac{\partial(Jf)}{\partial \xi} d\eta \right| = \left| \int_N g^2 \frac{1}{J} \frac{\partial(Jf)}{\partial \xi} \right| \leq c' \int_\Omega g^2$$

for some constant c'.

Combining the previous results we immediately prove the claim.

Q.E.D.

With this result we can show the following:

Lemma 2.

For any trial function Ψ that renders $\left|I[\Psi]\right|$ bounded by some given constant, the magnitude of each term in the numerator of Eqn. (4) is necessarily bounded by the denominator of Eqn. (4) times some constant that is independent of Ψ.

Proof:

Define

$$\zeta \equiv \frac{\int_\Omega \sigma|\nabla\vec{u}|^2 + \int_\Omega |\nabla\theta|^2 + \int_{\Omega_w} r\kappa_w|\nabla\theta_w|^2}{\int_\Omega |\vec{u}|^2 + \int_\Omega \theta^2 + \int_{\Omega_w} r\theta_w^2} ,$$

then

$$\begin{aligned}
&\frac{\int_{\partial\Omega} |\vec{u}|^2}{\int_\Omega |\vec{u}|^2 + \int_\Omega \theta^2 + \int_{\Omega_w} r\theta_w^2} \\
&= \frac{\int_{\partial\Omega} |\vec{u}|^2}{\int_\Omega |\vec{u}|^2} \cdot \frac{\int_\Omega |\vec{u}|^2}{\int_\Omega |\vec{u}|^2 + \int_\Omega \theta^2 + \int_{\Omega_w} r\theta_w^2} \\
&\leq \left(c_1 \sqrt{\frac{\int_\Omega |\nabla\vec{u}|^2}{\int_\Omega |\vec{u}|^2}} + c_2 \right) \cdot \frac{\int_\Omega |\vec{u}|^2}{\int_\Omega |\vec{u}|^2 + \int_\Omega \theta^2 + \int_{\Omega_w} r\theta_w^2} \\
&\leq c_1 \sqrt{\frac{\int_\Omega |\nabla\vec{u}|^2}{\int_\Omega |\vec{u}|^2 + \int_\Omega \theta^2 + \int_{\Omega_w} r\theta_w^2}} + c_2 \ . \qquad (6)
\end{aligned}$$

Therefore, we have

$$\begin{aligned}
&-\zeta + \alpha_M \sqrt{\sigma} c_1 \sqrt{\zeta} + \alpha_M \sigma c_2 + 2\sqrt{\sigma R} \geq I[\Psi] \\
&\geq -\zeta - \alpha_M \sqrt{\sigma} c_1 \sqrt{\zeta} - \alpha_M \sigma c_2 - 2\sqrt{\sigma R} \ , \qquad (7)
\end{aligned}$$

where α_M denotes the maximum of $|\alpha|$, and we have also applied Cauchy-Schwarz inequality to the term $\int_\Omega u_z\theta$. This clearly shows that ζ must be bounded by some constant that is independent of the choice of Ψ as long as $\left|I[\Psi]\right|$ is bounded by

some given number. Eqn. (6) then tells us even the boundary term $\int_{\partial\Omega} |\vec{u}|^2$ is bounded, and our proof is complete.

Q.E.D.

With the help of Lemma 2, one can immediately derive the following[24]

Theorem 1.

The *ordered* eigenvalues of $\mathcal{L}$ are bounded from above, and they vary continuously with respect to changes of parameters α, κ_w,...etc. in the problem. (This means the eigenvalues don't appear or disappear into nowhere when we tune the parameters.) In addition, there are no accumulation points in the eigenvalue spectrum, and, therefore, there are only a finite number of eigenvalues that are greater than zero.

The variational principle gives us the following characterization of the most unstable mode λ_1:

$$\lambda_1 = \max_{\Psi} I[\Psi] \; . \tag{8}$$

In this work we will call the configuration associated with λ_1 the "ground state." With this characterization we can state the second variational principle now.

Variational Principle II.

The critical Rayleigh number R_C that makes λ_1 vanish is characterized by

$$\frac{1}{\sqrt{R_C}} = \max_{\Psi} \frac{2\int_\Omega u_z\theta}{\int_\Omega |\nabla\vec{u}|^2 + |\nabla\theta|^2 + \int_{\partial\Omega} \alpha|\vec{u}|^2 + \int_{\Omega_w} r\kappa_w|\nabla\theta_w|^2} \equiv J[\Psi] \; , \tag{9}$$

where we have absorbed $\sqrt{\sigma}$ into the definition of $\vec{u}$.

Proof:

At criticality we have $0 = \lambda_1 \geq I[\Psi]$. Our claim then follows from Eqn. (4).

Q.E.D.

Notice this is exactly what we derived in Chapter 1 (Cf: Eqn. (1.18) and the remarks following it). In fact, we can extract more information by looking directly at Eqn. (1): If we set the time dependence to zero (to correspond to the onset configuration), then we see that $\sqrt{R_C}$ is a generalized eigenvalue of

$$\mathcal{R}\Psi \equiv -\nabla^2\Psi + \begin{pmatrix} \nabla p \\ 0 \\ 0 \end{pmatrix} = \frac{1}{\Lambda}\hat{A}\Psi \ , \tag{10}$$

provided $\sqrt{\sigma}$ is absorbed into $\vec{u}$, as was mentioned above.

Let $\hat{D}$ be a 5×5 diagonal matrix whose diagonal elements are 1,1,1,1 and $r\kappa_w$, repectively. Then $\mathcal{R}$ is an invertible operator because $\hat{D}\mathcal{R}$ is positive definite in the inner product defined above. If we now define a second inner product

$$\langle \Psi' | \Psi \rangle_2 \equiv \left\langle \nabla\Psi' | \hat{D} | \nabla\Psi \right\rangle + \int_{\partial\Omega} \alpha \vec{u}'^* \cdot \vec{u} \ ,$$

then, after integration by parts, it is straightforward to show the operator $\mathcal{R}^{-1}\hat{A}$ is self-adjoint under the second inner product, and the eigenfunctions can be chosen

to be real, as will be done from now on. In fact, for a given eigenstate Ψ one finds

$$\begin{aligned}\Lambda &= \frac{\left\langle \Psi \left| \mathcal{R}^{-1}\hat{A} \right| \Psi \right\rangle_2}{\langle \Psi | \Psi \rangle_2} \\ &= \frac{2\int_\Omega u_z\theta}{\int_\Omega |\nabla\vec{u}|^2 + |\nabla\theta|^2 + \int_{\partial\Omega}\alpha|\vec{u}|^2 + \int_{\Omega_w} r\kappa_w|\nabla\theta_w|^2} \\ &\equiv J[\Psi]\ ,\end{aligned} \tag{11}$$

a result that is trivially true in view of Eqns. (9) and (10). Therefore, solving for R_C is equivalent to solving a self-adjoint eigenvalue problem $\Lambda\Psi = \mathcal{R}^{-1}\hat{A}\Psi$, and the existence, orthogonality and completeness of the eigenstates (under the second inner product) follow from standard arguments in the literature.[25] We mention in passing that the eigenvalues of $\mathcal{R}$ apparently come in pairs of opposite signs, and their corresponding eigenvectors differ only in θ and θ_w, which are negative to their counterparts. Whenever no confusion is possible we will also call the eigenfunction associated with $\max J[\Psi]$ the "ground state."

Although we have formulated the problem with a realistic sidewall in terms of two variational principles, sometimes one simply replaces the effects of the sidewall by a mathematically simpler boundary condition that takes the form

$$\frac{\partial\theta}{\partial n} + \beta\theta = 0\ . \tag{12}$$

Here β is an "effective thermal conductivity" of the sidewall that is introduced to simulate the influences of the sidewall on the convection problem. One usually allows β to vary on $\partial\Omega$. The reason one would like to adopt this boundary condition is several-fold: (1) It captures the basic underlying physics, (2) the

associated mathematical problem is "simplified" because the convection cell becomes self-governed, (3) it admits comparison with the reaction-diffusion models of developmental biology, and (4) the case of negative β can be treated without modifications if we are interested in the behavior of the growth rate λ_j. (Later on I will show that the negative β regime, though never realizable in nature, turns out to be a convenient bypass for studying the more relevant regime with positive β.) The variational principles corresponding to a system subject to this "surrogate boundary condition" apparently will still look the same except for the following minor modifications:

$$\begin{aligned} &\int_{\Omega_w} \theta_w^2 \to 0 \\ &\int_{\Omega_w} r\kappa_w |\nabla\theta_w|^2 \to \int_{\partial\Omega} \beta\theta^2 \ . \end{aligned} \tag{13}$$

We will attach a superscript SBC to the two functionals $I[\cdots]$ and $J[\cdots]$ when we are considering a system with the surrogate boundary condition. The trial function for it will be denoted by ψ since θ_w is not involved. The associated linear operators will be denoted by $\mathcal{L}^{SBC}$ and $\mathcal{R}^{SBC}$, respectively. When the sidewall is perfectly conducting, instead of literally treating β as ∞, we should put in by hand the extra constraint that the trial function ψ must satisfy $\theta = 0$ on the sidewall. A physically appealing argument why this is so will be given in the next section.

Later we shall also investigate in what sense this surrogate boundary condition captures the underlying physics and simulates the sidewall properties.

§2.2 Some Monotonicity Results:

The variational principles readily allow one to derive the monotonic dependence of the stability on some of the adjustable parameters of the system. The following says the system is more stable if the boundary is "more viscous":

Theorem 2.

The eigenvalues λ_j and Λ_j $(j = 1, 2, ...)$ are both decreasing functions of α.

Proof:

We will prove it for λ_j only, because the proof for Λ_j is similar. Suppose Ψ is the ground state for a system with parameter α, and add a subscript α to $I[\cdots]$ to remind ourselves its explicit dependence on α, then

$$\begin{aligned}\lambda_1 = I_\alpha[\Psi] &= (I_\alpha[\Psi] - I_{\alpha'}[\Psi]) + I_{\alpha'}[\Psi] \\ &= -\frac{\int_{\partial\Omega} \sigma(\alpha - \alpha')|\vec{u}|^2}{\int_\Omega |\vec{u}|^2 + \int_\Omega \theta^2 + \int_{\Omega_w} r\theta_w^2} + I_{\alpha'}[\Psi] \\ &\leq -\frac{\int_{\partial\Omega} \sigma(\alpha - \alpha')|\vec{u}|^2}{\int_\Omega |\vec{u}|^2 + \int_\Omega \theta^2 + \int_{\Omega_w} r\theta_w^2} + \lambda_1'\end{aligned}$$

by the first variational principle, where primed quantities refer to those associated with α'. This clearly proves our claim for λ_1. We can then resort to Courant's minimum-maximum principle[24] to show that it is true for all λ_j.

Q.E.D.

The same trick can be exploited to show

Theorem 3.

The *ground state* growth rate λ_1 is an increasing function of the Rayleigh number R.

Proof:

Apparently, we only need to show that $\int_\Omega u_z\theta$ is greater than zero for the ground state. But if this were not the case we could simply flip the signs of θ and θ_w and show that the new trial function renders a bigger $I[\Psi]$, thus contradicting the variational characterization for λ_1. (Cf: Eqn. (8))

Q.E.D.

I should remark that this monotonicity property for λ_1 doesn't necessarily hold for other eigenvalues, as is demonstrated in Appendix A.

Theorem 4.

Everything else fixed, the onset Rayleigh number R_C increases if we make the sidewall thicker.

Proof:

Let the ground state for the system with a thicker wall be denoted by Ψ. We can construct a trial function Ψ' for the system with a thinner wall by restricting Ψ on $\Omega + \Omega'_w$. Quantities associated with the smaller system will be primed. Then,

$$\sqrt{R_C} = 1/J[\Psi] = (1/J'[\Psi']) + \frac{\int_{\Omega_w\setminus\Omega'_w} r\kappa_w|\nabla\theta_w|^2}{2\int_\Omega u_z\theta}$$
$$\geq \sqrt{R'_C} + \left(\frac{\int_{\Omega_w\setminus\Omega'_w} r\kappa_w|\nabla\theta_w|^2}{2\int_\Omega u_z\theta}\right) .$$

The theorem is true because $(\cdots)$ is positive.

Q.E.D.

Similarly, from Variational Principle I we can show

Theorem 5.

If the Rayleigh number is tuned so that λ_1 for the cell with a thicker wall is nonnegative, then the cell with a thinner wall satisfies $\lambda_1' \geq \lambda_1$.

It is interesting to note that for a vibrating membrane which satisfies the Neumann boundary condition one cannot prove a similar result like this for the first excited state because the eigenvalues of all the excited states have the same sign.

If we modify the previous argument slightly, so that the jump condition in Eqn. (1.12) is satisfied when we compare two systems that are in every respect the same except that their sidewall thermal conductivities are different, then Variational Principles I and II imply

Theorem 6.

λ_j is a decreasing function of the sidewall conductivity κ_w, whereas R_C is an increasing function of κ_w.

Clearly, Theorem 6 also holds for a surrogate system if we replace $r\kappa_w$ by the effective conductivity β. A moment's reflection shows that as long as we are

considering λ_j, we don't have to restrict ourselves to the case $\beta \geq 0$, *i.e.*, β can be negative without affecting our argument. What is interesting in this case is that we then have an apparent paradox: physically we expect the two cases $\beta = \pm\infty$ to correspond to the same situation in which the sidewall is a perfect thermal conductor. Yet Theorem 6 seems to indicate otherwise because the eigenvalues are predicted to be monotonically increasing (and, thus, never come back to their original values) when we tune β from $+\infty$ to $-\infty$. The apparent inconsistency is easily resolved once we realize that this is just the manifestation of the well-known phenomenon of holonomy in differential geometry[26] or "Berry's phase" in quantum mechanics[27], *i.e.*, cyclic evolution of a system doesn't necessarily bring the eigenstates of an operator on the system back to their starting configuration. As will be shown in the next section, some eigenvalues actually disappear into infinity when we vary β from $+\infty$ to $-\infty$. Fig. 2.2 shows schematically what happens for this cyclic evolution when β is treated like the angular coordinate on a cylinder and the two extremes $\beta = \pm\infty$ are identified.

The reason why we can only take trial functions whose θ vanishes on $\partial\Omega$ for a cell with perfectly conducting sidewalls in the variational formulation should be clear now: as we tune β_1 of $\theta + \beta_1 \frac{\partial\theta}{\partial n} = 0$ from 0^- to 0^+, several solutions are lost abruptly, and the numbering of the eigenstates is not preserved in this process. We would expect a result similar to Theorem 1 to hold if it were possible to construct a variational principle that is valid for β_1 in any open interval containing 0, thus

allowing the use of trial functions whose θ doesn't necessarily vanish on $\partial\Omega$.

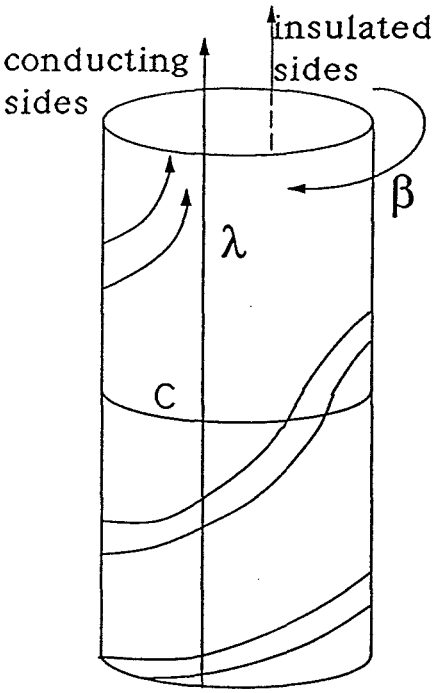

Figure 2.2: Schematic plot of eigenvalues λ_j as functions of β when the two extremes β=–infinity and β=infinity are identified on a cylinder. The ring c corresponds to a state that is never perturbed by β.

§2.3 The "Run-Away" Solution:

In this section we give a brief description of what happens when the effective thermal conductivity β of a surrogate system is tuned negative. This problem is of interest because later I will use this unphysical regime to derive properties for a surrogate system with a positive β.

Theorem 7.

Keep everything else other than β fixed. Then at least one eigenvalue λ_1 goes to $+\infty$ when the β on the sidewalls tends to $-\infty$. A similar result holds when we tune α to $-\infty$.

Proof:

Let's take a trial function whose temperature θ doesn't vanish on part of the sidewall and allow β to go to $-\infty$. Inspecting the expressions for $I^{SBC}[\psi]$ (Cf: Eqns. (4) and (13)) and Eqn. (8) we see $\lambda_1 \geq I_\beta^{SBC}[\psi] \to +\infty$ as β tends to $-\infty$. This proves our claim. The proof for α is similar.

Q.E.D.

Note: Apparently, symmetries are preserved in the foregoing argument. This means there is at least one "run-away" eigenfunction of the kind described above for solutions associated with each type of symmetry.

It is interesting to note that the above run-away eigenfunctions manage to disappear without jeopardizing the completeness of the whole set of eigenfunctions by mimicking a zero vector ψ=0 when β approaches $-\infty$. This mimicry is achieved by developing a very thin thermal boundary layer near the sidewalls and suppressing the velocity field in the fluid. In fact, this feature can be derived and the boundary layer width calculated very easily: first, we notice the term $\sqrt{\sigma R}u_z$ in Eqn. (1) must be much smaller than $\lambda_1\theta$ in magnitude, because otherwise $\sqrt{\sigma R}\theta\hat{e}_z$ would become negligible compared to other terms in the $\frac{\partial \vec{u}}{\partial t}$ equation, thus implying the

decoupling of the temperature and velocity fields. But then a restricted version of Eqn. (7) applied to the decoupled linearized Navier-Stokes equation alone immediately tells us λ_1 is bounded above and could never be made arbitrarily large when we tune β to $-\infty$, thus contradicting our assumption. This argument apparently implies velocity is suppressed strongly and is much smaller than the temperature everywhere in the cell.

Next, we "dot" the θ equation of Eqn. (1) by θ, and integrate over the whole cell to yield

$$-\int_\Omega |\nabla\theta|^2 + \int_{\partial\Omega} \theta\frac{\partial\theta}{\partial n} + \sqrt{\sigma R}\int_\Omega \theta u_z = \lambda\int_\Omega |\theta|^2 \ , \tag{14}$$

from which the presence of a thermal boundary layer is obvious because (i) the first term on LHS is always negative, and (ii) the third term is negligible compared to RHS. Thus, near the sidewall the θ equation can be approximated by

$$\frac{d^2\theta}{ds^2} \approx \lambda\theta \ , \tag{15}$$

where s is the inward normal distance away from the sidewall.

Solving Eqn. (15) subject to the boundary condition $-\frac{\partial\theta}{\partial s} + \beta\theta = 0$ yields

$$\theta \propto e^{\beta s} \tag{16}$$

and

$$\lambda \approx \beta^2 \ , \tag{17}$$

which clearly indicates a thermal boundary layer of width $\delta = -\frac{1}{\beta}$. The example studied in Appendix A (cf: Eqns. (A.12) and (A.13)) verifies our prediction.

The next proposition is intuitively obvious and follows from the continuity of solutions as functions of α.

Theorem 8.

The total number of run-away eigenfunctions when $\beta \to -\infty$ is independent of α as long as α is finite.

Because the *ordered* eigenfunctions for the rigid case are smoothly connected to the *ordered* solutions for the case $\frac{\partial \vec{u}_{\parallel}}{\partial n} + \alpha \vec{u}_{\parallel} = 0$ when $\alpha \to +\infty$, a continuity argument immediately sharpens Theorem 8 and gives, in particular,

Theorem 9.

The total number of run-away eigenfunctions as $\beta \to -\infty$ is the same for both rigid and free-slip cases.

Although Theorems 8 and 9 look quite innocent by themselves, a combination of both does produce the following less-expected assertion, which will find its use later.

Theorem 10.

Fix all the parameters except β. Assume λ_0 is a degenerate eigenvalue of multiplicity k when $\beta = \beta_0$ for some β_0. Then, no matter what value β takes, λ_0 is always an eigenvalue of multiplicity at least k-1, provided the total number of

run-away eigenfunctions is one when $\beta \to -\infty$. Again, we have a corresponding theorem for α.

Proof:

Arrange the eigenvalues in decreasing order and let the multiplicities of the eigenvalues be denoted by $n_1, n_2, n_3, \ldots$ In Fig. 2.3 we put in juxtaposition the ordering of eigenvalues for the three cases $\beta = \beta_0$ and $\beta = \pm\infty$ schematically. Monotonicity of eigenvalues with respect to β, *i.e.*, Theorem 6 for a surrogate system, is explicitly shown in the figure.

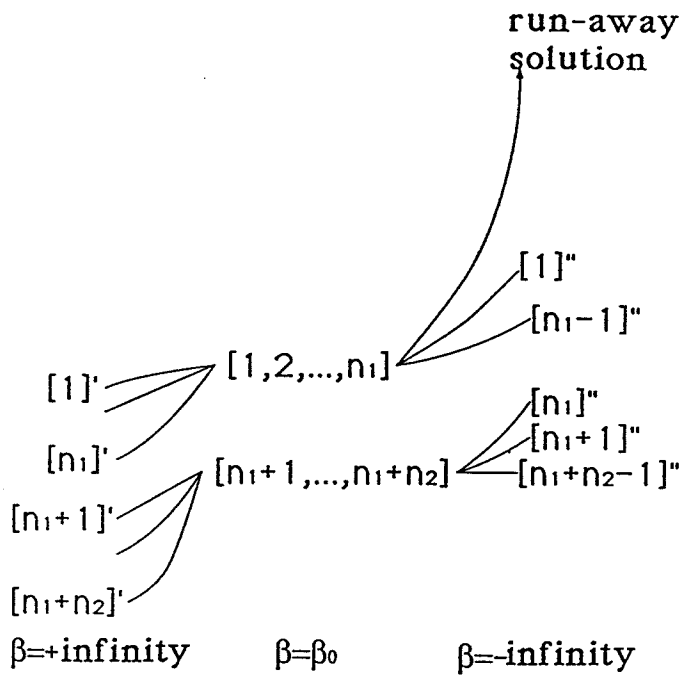

Figure 2.3: Monotonicity of λ_j with respect to β is shown with [...]' and [...]" denoting, respectively, the eigenvalues for β=infinity and β=−infinity.

From the figure we see that

$$[1]'' \geq \cdots \geq [n_1 - 1]'' \geq [1]' \tag{18}$$

$$[n_1 + 1]'' \geq \cdots \geq [n_1 + n_2 - 1]'' \geq [n_1 + 1]' \tag{19}$$

$$\vdots \quad ,$$

where [j] denotes the eigenvalue of the j-th state.

Since the two cases $\beta = \pm\infty$ correspond to the same physical problem of having a perfect conductor, we must have

$$[1]'' = [1]' \tag{20}$$

$$[n_1 + 1]'' = [n_1 + 1]' \, . \tag{21}$$

Combining Eqn. (18) with Eqn. (20) immediately shows there are at least $n_1 - 1$ states in the first group that can never change their eigenvalues when β varies. Similarly, inspection of Eqns. (19) and (21) tells us there is a degeneracy of at least $n_2 - 1$ in the second group, irrespective of what β is. Our claim can then be proved by induction.

Q.E.D.

I should point out that the previous proof respects the symmetries of the system, too. In other words, the assertion is still valid if we consider only solutions with specific symmetry. As a matter of fact, the theorem is only useful when we

can sort out the symmetries of the system first to guarantee the uniqueness of the run-away eigenfunction. An explicit application of this theorem will be given later when we investigate the size dependence of convection problems.

Chapter 3: Study Of The Surrogate System

We devote this chapter to the study of various properties of a surrogate system. First, I will develop a formal perturbation theory to deal with the change of stability when the sidewall properties are varied. By way of the proof of a particular theorem, I briefly touch upon the similarity and difference between a convection system and the reaction-diffusion model one usually encounters in developmental biology. Then, the influence of system size on the stability of this surrogate system is discussed *via* the combination of a perturbative approach and the results I derived in Chapter 2 based on the variational principles. This allows me to conclude, in particular, that the critical Rayleigh number for a large system with dimension L differs from its infinite cell limit by an amount that is proportional to L^{-2}. The last section of this chapter is devoted to the comparison of the surrogate system and a real convection cell, *i.e.*, one that has a realistic sidewall.

§3.1 Perturbation Theory, Size Dependence, And Biological Pattern Formation:

Let $\{|\psi_j>\}$ denote the orthonormal eigenvectors of $\mathcal{L}^{SBC}$ subject to the boundary conditions of Eqns. (1.13) through (1.15) and (2.12). The corresponding eigenvalue for $|\psi_j>$ is denoted by λ_j. For any given nondegenerate eigenvalue λ_0

we define the Green's function by

$$G_\lambda \equiv \sum_{j\neq 0} \frac{|\psi_j><\psi_j|}{\lambda_j - \lambda} \ . \tag{1}$$

If we use a prime to denote variables associated with the different thermal boundary condition $\frac{\partial\theta'}{\partial n} + \beta'\theta' = 0$, then Lyapunov-Schmidt reduction of $\mathcal{L}\psi' = \lambda'\psi'$ immediately gives

$$(\lambda' - \lambda_0)\int_\Omega {\psi_0}^\dagger \psi' = \int_{\partial\Omega} {\psi_0}^\dagger \frac{\partial\psi'}{\partial n} - \frac{\partial{\psi_0}^\dagger}{\partial n}\psi' = -\int_{\partial\Omega}(\beta' - \beta){\psi_0}^\dagger \hat{B}\psi' \ , \tag{2}$$

$${\psi'}^\perp = \int_{\partial\Omega}(\beta' - \beta)G_{\lambda'}\hat{B}\psi' \ , \tag{3}$$

$$\psi' \equiv \psi_0 + {\psi'}^\perp \ , \tag{4}$$

where $\hat{B}$ is a 4×4 matrix with only one nonvanishing element $B_{44} = 1$, and ${\psi'}^\perp$ is the projection of ψ' off the one-dimensional subspace spanned by ψ_0. From the known solutions (ψ_j, λ_j), one can compute (ψ', λ') by the following iteration scheme whose convergence can be established by standard methods, provided $|\beta' - \beta|$ is small enough:

$$\begin{aligned}
\lambda'^{(1)} - \lambda_0 &= -\int_{\partial\Omega}(\beta' - \beta)\psi_0^\dagger \hat{B}\psi_0 \ , \\
{\psi'}^{\perp(1)} &= \int_{\partial\Omega}(\beta' - \beta)G_{\lambda_0}\hat{B}\psi_0 \ , \\
\lambda'^{(l+1)} - \lambda_0 &= -\int_{\partial\Omega}(\beta' - \beta)\psi_0^\dagger \hat{B}\psi'^{(l)} \ , \qquad (l \geq 1) \\
{\psi'}^{\perp(l+1)} &= \int_{\partial\Omega}(\beta' - \beta)G_{\lambda'^{(l)}}\hat{B}\psi'^{(l)} \ , \\
\psi'^{(l)} &\equiv \psi_0 + {\psi'}^{\perp(l)} \ .
\end{aligned} \tag{5}$$

Notice the first equation implies $\frac{\partial\lambda}{\partial\beta} = -\frac{\int_{\partial\Omega}|\theta|^2}{\int_\Omega |\vec{u}|^2+|\theta|^2}$, a result that apparently is also derivable based on the variational principle. (Note: The proof of Theorem 2.1, when transcribed for variation of β instead of α, obviously gives us this result.)

When the two states ψ_1 and ψ_2 are nearly degenerate we can define a Green's function

$$G_\lambda \equiv \sum_{j\neq 1,2} \frac{|\psi_j><\psi_j|}{\lambda_j - \lambda} , \tag{1'}$$

and do Lyapunov-Schmidt reduction on the two-dimensional subspace spanned by ψ_1 and ψ_2 to obtain

$$\begin{pmatrix} \lambda_1 - \lambda' - b_{11} & -b_{12} \\ -b_{21} & \lambda_2 - \lambda' - b_{22} \end{pmatrix} \begin{pmatrix} x_1 \\ x_2 \end{pmatrix} = \begin{pmatrix} \int_{\partial\Omega}(\beta' - \beta)\psi_1^\dagger \hat{B}\psi'^\perp \\ \int_{\partial\Omega}(\beta' - \beta)\psi_2^\dagger \hat{B}\psi'^\perp \end{pmatrix}, \tag{2'}$$

$$\psi'^\perp = \int_{\partial\Omega} (\beta' - \beta) G_{\lambda'} \hat{B}\psi' , \tag{3'}$$

$$\psi' \equiv x_1\psi_1 + x_2\psi_2 + \psi'^\perp , \tag{4'}$$

$$b_{ij} \equiv \int_{\partial\Omega} (\beta' - \beta)\psi_i^\dagger \hat{B}\psi_j . \tag{6}$$

This suggests the following iteration scheme for solving for (ψ_1', λ_1') and (ψ_2', λ_2'):

(1) Lowest order eigenvalue $\lambda'^{(1)}$ is to be obtained by solving

$$\begin{pmatrix} \lambda_1 - \lambda'^{(1)} - b_{11} & -b_{12} \\ -b_{21} & \lambda_2 - \lambda'^{(1)} - b_{22} \end{pmatrix} \begin{pmatrix} x_1^{(1)} \\ x_2^{(1)} \end{pmatrix} = 0 . \tag{7}$$

This also determines

$$\frac{x_2^{(1)}}{x_1^{(1)}} = \frac{b_{22} - b_{11} + \lambda_1 - \lambda_2 \pm \sqrt{(b_{11} - b_{22} + \lambda_2 - \lambda_1)^2 + 4b_{12}b_{21}}}{2b_{12}} , \tag{8}$$

where we have assumed $b_{12} \neq 0$ for simplicity. Our normalization convention can then be taken as $x_1 \equiv 1$.

(2) Iteration:

$$\psi'^{\perp(1)} \equiv 0$$

$$\begin{pmatrix} \lambda_1 - \lambda'^{(l+1)} - b_{11} & -b_{12} \\ -b_{21} & \lambda_2 - \lambda'^{(l+1)} - b_{22} \end{pmatrix} \begin{pmatrix} 1 \\ x_2^{(l+1)} \end{pmatrix} = \begin{pmatrix} \int_{\partial\Omega} (\beta' - \beta) \psi_1^\dagger \hat{B} \psi'^{\perp(l)} \\ \int_{\partial\Omega} (\beta' - \beta) \psi_2^\dagger \hat{B} \psi'^{\perp(l)} \end{pmatrix}$$

$$\psi'^{\perp(l+1)} = \int_{\partial\Omega} (\beta' - \beta) G_{\lambda'^{(l)}} \hat{B} \psi'^{(l)}$$

$$\psi'^{(l)} \equiv \psi_1 + x_2^{(l)} \psi_2 + \psi'^{\perp(l)} \ , \tag{5'}$$

where $x_2^{(l+1)}$ and $\lambda'^{(l+1)}$ are solved by the matrix equation shown above.

Recall that we showed in Theorem 2.10 that sometimes it is possible for an eigenvalue to remain the same no matter how β is varied. This rare occurrence apparently imposes a very strong constraint because it requires θ (and $\frac{\partial\theta}{\partial n}$, in view of (2.12)) to vanish identically on the sidewalls, irrespective of what value β assumes. As a matter of fact, Eqn. (5) or (5') implies an even stronger assertion:

Theorem 1.

If both θ and $\frac{\partial\theta}{\partial n}$ ever become identically zero on the sidewalls for some β, then the eigenstate and the eigenvalue will never be perturbed by β at all. Similar results hold for perturbation by α.

Proof:

For the nondegenerate case we can use Eqn. (5) and check that the eigenstate and the eigenvalue remain the same up to any order of iteration. In the case when degeneracy happens one can resort to either a continuity argument or straightforward degenerate perturbation, Eqn. (5′), to prove our claim.

Q.E.D.

Perturbation theory can also be applied to studying the size dependence of the stability of a cell whose sidewall is smooth, rigid, and perfectly conducting. Let's assume Ω' is a cell that is completely inside a slightly bigger cell Ω. A Lyapunov-Schmidt reduction yields

$$(\lambda' - \lambda_0) = \frac{\int_{\partial\Omega'} \psi_0^\dagger \hat{D} \frac{\partial \psi'}{\partial n}}{\int_{\Omega'} \psi_0^\dagger \psi'} , \tag{9}$$

$$\psi'^{\perp} = -\int_{\partial\Omega'} G_{\lambda_0} \hat{D} \frac{\partial \psi'}{\partial n} , \tag{10}$$

where we have extended the definition of ψ' by setting $\psi' \equiv 0$ outside Ω', and $\psi' \equiv \psi_0 + \psi'^{\perp}$. Here, $\partial\Omega'$ refers to the sidewall alone, and notice the integral is over Ω'. These equations suggest the following iteration scheme for solving the solutions for Ω' :

$$\begin{aligned}
\lambda'^{(1)} - \lambda_0 &= \frac{\int_{\partial\Omega'} \psi_0^\dagger \hat{D} \frac{\partial \psi_0}{\partial n}}{\int_{\Omega'} \psi_0^\dagger \psi_0} , \\
\psi'^{\perp(1)} &= -\int_{\partial\Omega'} G_{\lambda_0} \hat{D} \frac{\partial \psi_0}{\partial n} , \\
\lambda'^{(l+1)} - \lambda_0 &= \frac{\int_{\partial\Omega'} \psi_0^\dagger \hat{D} \frac{\partial \psi'^{(l)}}{\partial n}}{\int_{\Omega'} \psi_0^\dagger \psi'^{(l)}} , \\
\psi'^{\perp(l+1)} &= -\int_{\partial\Omega'} G_{\lambda_0} \hat{D} \frac{\partial \psi'^{(l)}}{\partial n} .
\end{aligned} \tag{11}$$

Now we can prove a monotonicity result.

Theorem 2.

Let Ω and Ω' be two cells whose sidewalls are smooth, rigid, and perfectly conducting. Assume Ω' is completely inside Ω and it is possible to smoothly transform $\partial\Omega$ to $\partial\Omega'$, then $\lambda_j > \lambda'_j$ for j=1,2.... In other words, Ω' is strictly more stable than Ω. (Notice that this result can be trivially translated in terms of R_c by virtue of Theorem 2.3.)

Proof:

It suffices to prove this statement when the cells almost coincide. We will also assume, without real loss of generality, that the state we are considering is nondegenerate.

If $\frac{\partial\psi_0}{\partial n}$ is not identically zero on $\partial\Omega$, then the lowest order iteration of Eqn. (11) yields

$$\lambda'^{(1)} - \lambda_0 = \frac{\int_{\partial\Omega'} \psi_0^\dagger \hat{D} \frac{\partial\psi_0}{\partial n}}{\int_{\Omega'} \psi_0^\dagger \psi_0} \approx -\int_{\partial\Omega} \frac{\partial\psi_0^\dagger}{\partial n} \hat{D} \frac{\partial\psi_0}{\partial n} \mathrm{s} < 0 \ ,$$

where s is the inward normal distance from a point on $\partial\Omega$ to $\partial\Omega'$. This clearly proves our claim. So there remains the possibility that $\frac{\partial\psi_0}{\partial n}$=0 on $\partial\Omega$. If this happens, then next order iteration of Eqn. (11) yields

$$\lambda'^{(2)} - \lambda_0 = \frac{\int_{\partial\Omega'} \psi_0^\dagger \hat{D} \frac{\partial\psi'^{(1)}}{\partial n}}{\int_{\Omega'} \psi_0^\dagger \psi'^{(1)}} \approx -\int_{\partial\Omega} \frac{1}{2} \frac{\partial^2\psi_0^\dagger}{\partial n^2} \hat{D} \frac{\partial^2\psi_0}{\partial n^2} \mathrm{s}^3 \leq 0 \ .$$

But we claim that "=" is never attained in the above expression. In fact, the equality can hold only if $\psi_0 = \frac{\partial \psi_0}{\partial n} = \frac{\partial^2 \psi_0}{\partial n^2} = 0$ on the sidewall. Yet, upon rewriting the original fluid equations in local coordinates near the sidewall, one immediately arrives at the following initial value problem for fluid variables as functions of s:

$$\frac{\partial^2 \psi}{\partial s^2} = f_1 \ ,$$
$$\frac{\partial p}{\partial s} = f_2 \ ,$$

where f_1 and f_2 are "driving terms" that (i) only involve lower order derivatives in s and derivatives along the sidewall, and (ii) vanish identically on the sidewall if $\psi_0 = \frac{\partial \psi_0}{\partial n} = \frac{\partial^2 \psi_0}{\partial n^2} = 0$ on it. This implies $\psi \equiv 0$ inside Ω after integrating along s, thus contradicting our assumption that ψ is an eigenvector. Therefore, "=" can never be attained, and our proof is complete.

Q.E.D.

We note that a proof of this theorem based on the variational principle is no simpler because the trial function for the smaller domain must be carefully chosen to take care of the $\mathcal{O}(s^3)$ possibility we treated above if strict inequality is to be proved. Also note that although our proof assumes a smooth sidewall, thus excluding a rectangular cell, we can easily modify the proof to cover the case when the stability of two rectangular cells is to be compared. The idea is to compare them with an intermediate rectangular cell Ω'' whose two pairs of parallel sidewalls are each in contact with the sidewalls of Ω and Ω', respectively (see Fig. 3.1).

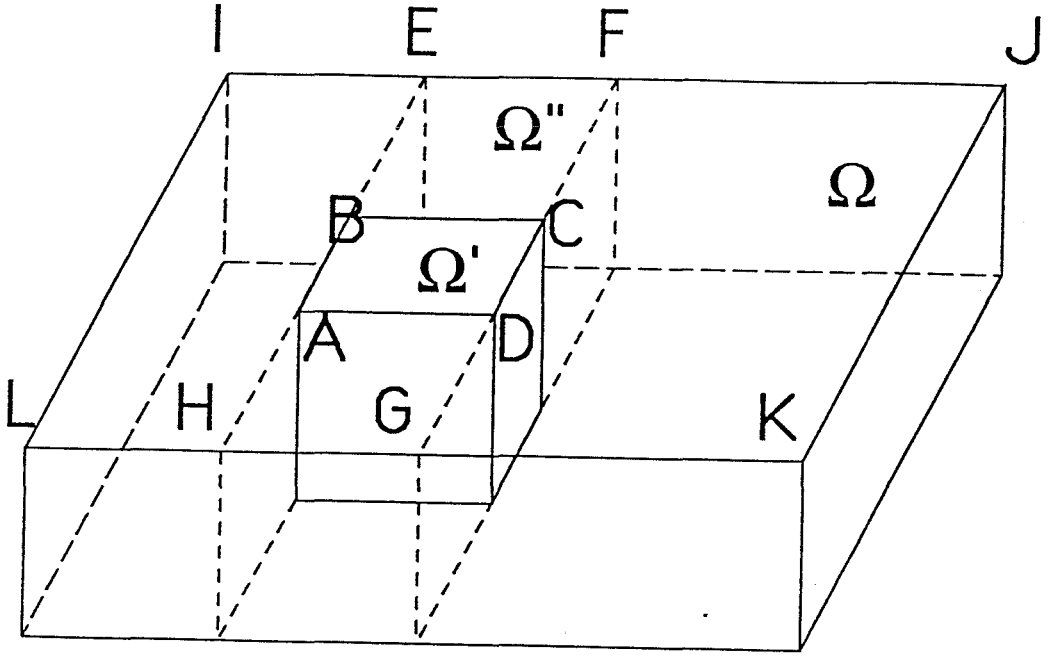

Figure 3.1: An intermediate cell Ω"=EFGH is introduced to allow one to compare stability of Ω'=ABCD and Ω=IJKL.

Theorem 3.

Let Ω be a rectangular box whose x dimension is L. Stretch Ω by a factor $l > 1$ in the x direction to obtain a larger box Ω'. Assume the boundary conditions for both boxes are:

(1) the two horizontal plates are rigid or free-slip, and perfectly conducting,

(2) $\frac{\partial \theta}{\partial n} + \beta\theta = 0$ $(\beta > 0)$ on the sidewalls, and

(3) $\vec{u}$=0 on the sidewalls.

Then there exists an l_1 such that $R_c^{\Omega'} < R_c^{\Omega}$ for all $l > l_1$.

Proof:

If θ happens to be identically zero on the sides that are parallel to the $y-z$ plane, then a modified version of Theorem 2 implies any l_1 greater than 1 will do. Thus, we can assume θ doesn't vanish identically on them. We now try to fill up Ω' by placing side by side as many copies of Ω as possible. In general there will be a gap Ω_g left that is too small for any copy of Ω to be put in (see Fig. 3.2). Assume it takes N copies $\Omega_1, \Omega_2, ..., \Omega_N$ to almost fill Ω'.

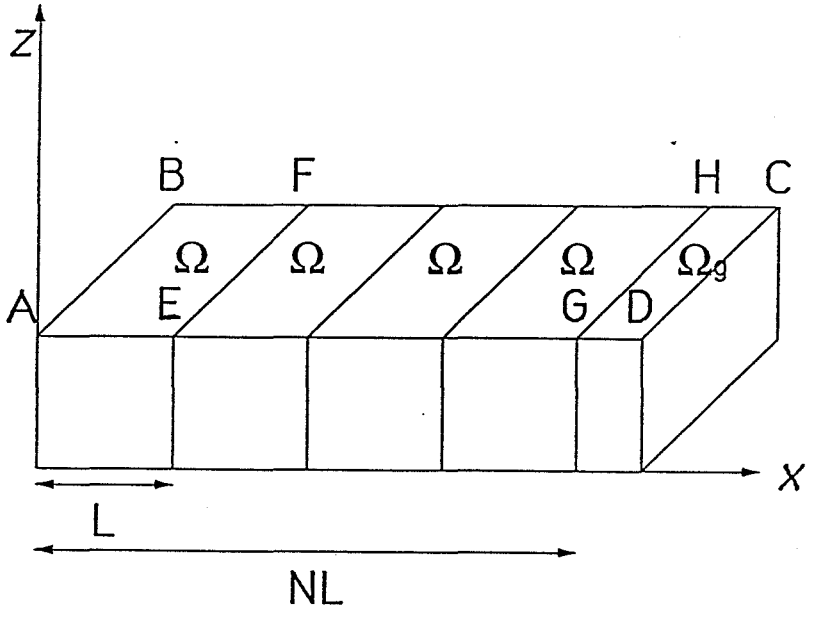

Figure 3.2: N copies of identical box Ω are joined lengthwise to fill up cell Ω'=ABCD, with an unfilled gap Ω_g.

We construct a trial function ψ' for Ω' in the following manner:

(1) Inside each of $\Omega_1, \Omega_3, \Omega_5, ...$ we simply take the ground state wavefunction ψ of Ω as ψ'.

(2) Inside each of $\Omega_2, \Omega_4, \Omega_6, \ldots$ we define ψ' to be the reflection of ψ with respect to the wall common to its neighboring cell.

(3) In the gap Ω_g we define ψ' as $\vec{u}' \equiv 0$ and $\theta'(x,y,z) \equiv \theta(NL,y,z)$.

Note that the "kinks" of ψ' across the cell walls can be smoothed and present no real difficulty to our argument. Thus,

$$\begin{aligned} J^{\Omega}[\psi] &= \frac{N(\int_{\Omega} |\nabla \vec{u}|^2 + |\nabla\theta|^2) + N\int_{\partial\Omega} \beta|\theta|^2}{2N\int_{\Omega} u_z\theta} \\ &= \frac{\int_{\Omega'} |\nabla \vec{u}'|^2 + |\nabla\theta'|^2 + \int_{\partial\Omega'} \beta|\theta'|^2 + N\int_{\partial\Omega} \beta|\theta|^2}{2\int_{\Omega'} u_{z'}\theta'} + \mathcal{O}(\frac{1}{N}) \\ &= J^{\Omega'}[\psi'] + \frac{\int_{\partial\Omega} \beta|\theta|^2}{2\int_{\Omega} u_z\theta} + \mathcal{O}(\frac{1}{N}) \, . \end{aligned} \tag{12}$$

By the second variational principle we see this implies $R_C^{\Omega} > R_C^{\Omega'}$ for all large enough N.

Q.E.D.

It is obvious that we can easily modify the proof and replace condition (3) of the previous theorem by the more general viscous boundary condition $\frac{\partial \vec{u}_{\|}}{\partial n} + \alpha \vec{u}_{\|} = 0$ with $\alpha > 0$. The same is true if the larger box is large in both x and y directions. The main point to be made in theorems of this type apparently lies in Eqn. (12) and the like which says *the finite system is more stable than an infinite system by an amount that is about what the boundary contributes in the variational expression for* R_C.

A look at Fig. A.3 shows that our inability to prove strict monotonicity for all Ω' bigger than Ω stems from the fact that oscillatory behavior does indeed

exist when Ω' is not too much bigger than Ω. This oscillation can be viewed as the remnant of a very special spatial pattern selection mechanism one often encounters in the reaction-diffusion models of developmental biology. To see the connection between the two, we recall in the study of biological pattern formation that one usually analyzes the stability of the following model[28] :

$$\hat{D}\nabla^2\psi + \hat{A}\psi = \lambda\psi \qquad \text{in } \Omega \,, \tag{13}$$

$$\hat{D}\frac{\partial\psi}{\partial n} + \hat{B}\psi = 0 \qquad \text{on } \partial\Omega, \tag{14}$$

where $\psi \in \mathcal{C}^{\mathrm{m}}$ is an m-component concentration field in a "cell" Ω, $\hat{D}, \hat{A}$, and $\hat{B}$ are $m \times m$ matrices. Usually $\hat{D}$ is positive definite and $\hat{B}$ is identically zero.

The problem can be solved analytically for the no-flux boundary condition by taking the solution to be of form

$$\psi = \varphi\bar{\psi} \,, \tag{15}$$

where $\bar{\psi}$ is some $m \times 1$ constant vector, and φ is an eigenfunction of Laplacian subject to the Neumann boundary condition:

$$\nabla^2\varphi = \mu\varphi \qquad \text{in } \Omega \,, \tag{16}$$

$$\frac{\partial\varphi}{\partial n} = 0 \qquad \text{on } \partial\Omega \,. \tag{17}$$

Substituting Eqn. (15) into Eqn. (13) we get the dispersion relation

$$det(\mu\hat{D} + \hat{A} - \lambda) = 0 \,. \tag{18}$$

When the control parameters in the matrix $\hat{A}$ are suitably adjusted, there will only be one branch of solution that becomes marginally stable when μ equals some value μ_c. For all other μ the associated λ will have a negative real part and corresponds to a stable configuration. Because μ scales in size L like L^{-2}, a cell that expands indefinitely will lower the μ of each mode, thus allowing different modes to become unstable, in turn, upon passage through μ_c, only to recover their stability after further expansion. A plot of the growth rate λ versus L for this scenario looks very much like Fig. A.1(a).

For a convection cell with free-slip boundaries and insulating sidewalls the most natural ansatz is to write the solution ψ to the problem as

$$\psi \equiv \begin{pmatrix} u_x \\ u_y \\ u_z \\ \theta \end{pmatrix} = \begin{pmatrix} \bar{u}\frac{\partial \varphi}{\partial x} \\ \bar{u}\frac{\partial \varphi}{\partial y} \\ \bar{u}_z\frac{\partial \varphi}{\partial z} \\ \bar{\theta}\frac{\partial \varphi}{\partial z} \end{pmatrix}, \qquad (19)$$

$$p = \bar{p}\varphi,$$

where $\bar{u}, \bar{u}_z, \bar{\theta}$ and $\bar{p}$ are constants to be determined, and φ satisfies Eqns. (16) and (17).

Upon substitution of Eqn. (19) into the governing equations, one obtains

$$\begin{pmatrix} -1 & \sigma\mu - \lambda & 0 & 0 \\ -1 & 0 & \sigma\mu - \lambda & \sqrt{\sigma R} \\ 0 & 0 & \sqrt{\sigma R} & \mu - \lambda \\ 0 & \mu - \mu_z & \mu_z & 0 \end{pmatrix} \begin{pmatrix} \bar{p} \\ \bar{u} \\ \bar{u}_z \\ \bar{\theta} \end{pmatrix} = 0 , \qquad (20)$$

where we have separated out z-dependence by introducing $\frac{\partial^2 \varphi}{\partial z^2} \equiv \mu_z \varphi$ for some appropriate constant μ_z. Solving Eqn. (20) for λ we get

$$\frac{\lambda}{\mu} = \frac{1 + \sigma \pm \sqrt{(1+\sigma)^2 - 4\sigma(1 - \frac{R}{\mu^2}(1 - \frac{\mu_z}{\mu}))}}{2} , \qquad (21)$$

from which we see that the pattern selection mechanism described before for biological systems works equally well here if we tune R to $R_{C0} \equiv \min \frac{\mu^3}{\mu - \mu_z}$.

Unfortunately, this particular case turns out to be more complicated than is described above! The problem is that this trick requires the vertical vorticity of the eigenfunctions we are interested in to vanish. Yet this is not guaranteed for the problem at hand.* But for a one-dimensional problem this complication apparently doesn't occur, and in Fig. A.1(a) I show the λ versus L plot for it when $R = R_{C0} = \frac{27}{4}\pi^4$. One feature worth noticing in this figure is that there are many intersections among different modes. When we change the viscous and/or thermal properties on the sidewalls the intersections generally will break up and form many oscillations, as shown in Fig. A.1(b). This clearly justifies our calling the wavy curves remnants of a special biological pattern selection mechanism. The implication is that Rayleigh-Bénard convection can be thought of as a canonical pattern formation problem bearing features that some more specialized reaction-diffusion models possess.

I should point out that a large three-dimensional cell whose two horizontal plates satisfy the more general boundary condition, Eqn. (1.15), with a positive α or the physically realizable rigid condition *can* actually be solved by similar ansatz

* See Appendix B for a discussion of the subtlety involved.

if the sidewall is free-slip and perfectly insulating:*

$$\psi = \begin{pmatrix} \bar{u}\frac{\partial\varphi}{\partial x} \\ \bar{u}\frac{\partial\varphi}{\partial y} \\ \bar{u}_z\varphi \\ \bar{\theta}\varphi \end{pmatrix} , \qquad p = \bar{p}\varphi \ . \tag{22}$$

Here, φ is the eigenfunction of two-dimensional Laplacian on the horizontal cross-section of the cell subject to the Neumann boundary condition, and $\bar{u}$, $\bar{u}_z$, $\bar{\theta}$ and $\bar{p}$ are functions of z properly chosen so that the governing equations and the boundary conditions at $z = 0, 1$ are satisfied.

Albeit our showing the similarity of pattern generation between convection and biological systems, there exists a difference in which incompressibility of fluid plays some role, as the next theorem and the remarks following it show.

Theorem 4.

Consider the eigenvalue problem of Eqns. (13) and (14), in which $\hat{A}$ is self-adjoint and $\hat{B}$ is positive semidefinite. If Ω' is a cell obtained by linearly stretching Ω in the x direction by a factor $l > 1$, then $\lambda'_j \geq \lambda_j$ for all j.

Proof:

The eigenvalue problem is equivalent to the variational principle of the following functional:

$$K^{\Omega}[\psi] \equiv \frac{-\int_\Omega \nabla\psi^\dagger \hat{D}\nabla\psi + \int_\Omega \psi^\dagger \hat{A}\psi - \int_{\partial\Omega} \psi^\dagger \hat{B}\psi}{\int_\Omega \psi^\dagger\psi} \ .$$

* This is in sharp contrast to the case when α is zero. The validity of this method is verified in Appendix B.

Let's assume $\psi(x,y,z)$ is the "ground state" for the cell Ω. Hence, $\lambda_1 = K^{\Omega}[\psi]$. Next, we define a trial function ψ' for the stretched domain Ω' as $\psi'(x',y',z') \equiv \psi(\frac{x'}{l},y',z')$.

For any function $f(x,y,z)$, we have

$$\begin{aligned}\int_{\Omega} f(x,y,z)dxdydz &= \frac{1}{l}\int_{\Omega'} f(\frac{x'}{l},y',z')dx'dy'dz' \\ &\equiv \frac{1}{l}\int_{\Omega'} f' ,\end{aligned}$$

where $f'(x',y',z') \equiv f(\frac{x'}{l},y',z')$.

Similarly,

$$\int_{\Omega} \frac{\partial\psi^{\dagger}}{\partial x}\hat{D}\frac{\partial\psi}{\partial x} = l^2 \cdot \frac{1}{l}\int_{\Omega'} \frac{\partial\psi'^{\dagger}}{\partial x'}\hat{D}\frac{\partial\psi'}{\partial x'} .$$

We also have

$$\int_{\partial\Omega} f = \int\int \frac{f}{\cos\theta}dydz = \int_{\Omega'} f'\frac{\cos\theta'}{\cos\theta} ,$$

where θ (θ') is the angle between the surface area element of $\partial\Omega$ ($\partial\Omega'$) and the y-z plane. Hence, $l\int_{\partial\Omega} f = \int_{\partial\Omega'} f' l\frac{\cos\theta'}{\cos\theta}$. But from Fig. 3.3 we readily see

$$l\frac{\cos\theta'}{\cos\theta} = l\cdot\frac{\Delta s/\sqrt{(\Delta s)^2+(l\Delta x)^2}}{\Delta s/\sqrt{(\Delta s)^2+(\Delta x)^2}} > 1 ,$$

thus, $l\int_{\partial\Omega} f \geq \int_{\partial\Omega'} f'$, if f is nonnegative on $\partial\Omega$.

Combining all the previous results one obtains

$$\begin{aligned}\lambda_1 &= K^{\Omega}[\psi] \\ &\leq \frac{-\int_{\Omega'}\nabla'\psi'^{\dagger}\hat{D}\nabla'\psi' + \int_{\Omega'}\psi'^{\dagger}\hat{A}\psi' - \int_{\partial\Omega'}\psi'^{\dagger}\hat{B}\psi'}{\int_{\Omega}'\psi'^{\dagger}\psi'} \\ &\leq \lambda_1' ,\end{aligned}$$

by the variational principle. Our claim can then be proved by invoking the minimum-maximum principle.

Q.E.D.

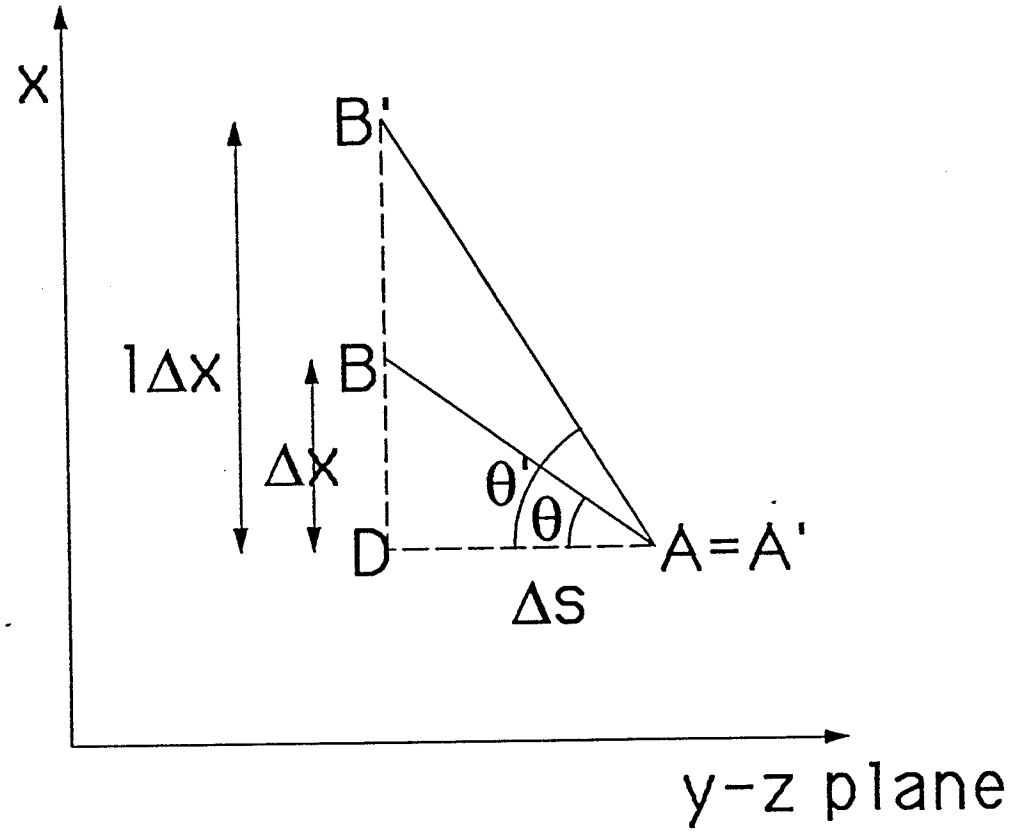

Figure 3.3: Side view of a small segment AB of the boundary of Ω and its stretched version A'B' on the boundary of Ω'. A and A' are identified for convenience.

A system that satisfies the conditions specified in the previous theorem, therefore, is not a candidate for biological pattern formation. After comparing Eqn. (13) and $\mathcal{L}^{SBC}\psi = \lambda\psi$, we see the major difference between the two pattern forming systems is the incompressibility condition. In fact, the role played by the incompressibility condition can be most easily appreciated by comparing the proofs of Theorems 2 and 3: in the former we have to put identical copies of Ω side by side

to produce a good trial function because the stability is lowered if an extra number of more or less identical convective rolls can be generated to fill up the additional space created due to the size increase, thus allowing the system to switch to a configuration of more rolls, while in the latter, incompressibility constraint is absent and "stretching" the original solution for Ω readily produces a solution of lower stability for the larger cell Ω', thus no switching to other modes is necessary.

We now concentrate on the scaling behavior of R_C when the cell dimension L varies from 0 to $+\infty$.

The small L behavior can be easily extracted from the fact that the critical Rayleigh number corresponding to other boundary conditions is no smaller than $\frac{\mu^3}{\mu-\mu_z}$, the critical Rayleigh number for the same cell with free-slip boundaries and insulating sidewalls, thanks to the analysis of Chapter 2. Thus,

$$R_C \geq \frac{\mu^3}{\mu - \mu_z} \propto \frac{1}{L^4} \tag{23}$$

for small L because μ scales like L^{-2}. We can also see this from Eqn. (2.9) because each of $\nabla\vec{u}$ and $\nabla\theta$ contributes a L^{-1} factor for small L.

I haven't been able to prove with complete rigor that for a large cell of arbitrary geometry the difference between R_C and its infinite cell limit $R_{C\infty}$ is of order L^{-2}, though a very plausible argument is presented below to show that this is indeed the case. The idea is to study a cylindrical cell first and then compare it to other cells of different geometry to derive the correct scaling behavior.

To motivate the reasoning for the physically more relevant case of having two rigid horizontal plates, let's first study only the states with zero vertical vorticity for a completely free-slip cylindrical cell with an insulating sidewall of radius L. We have, in cylindrical coordinates,

$$\varphi = \sin n\pi(z + \frac{1}{2}) \cdot e^{im\phi} J_m(k_{m,j}\frac{r}{L}) \ , \tag{24}$$

where m,n are integers, J_m is the Bessel function of order m, and $k_{m,j}$ is the j-th root to $\frac{dJ_m(\rho)}{d\rho} = 0$. The corresponding λ versus L curves for fixed m and n look very much like that shown in Fig. A.1 when $R = R_{C0}$. It is clear that at the intersection of any two curves we can find a state φ_1 in the two-dimensional degenerate subspace such that $\varphi_1 = \frac{\partial\varphi_1}{\partial r} = 0$ at r=L. This means the state satisfies $\theta = \frac{\partial\theta}{\partial r} = 0$ on the sidewall, thus implying it will never be perturbed by β from our previous discussions. We will call it an "anchored state" in what follows. In addition, this implies there is only one run-away solution when $\beta \to -\infty$. Hence, the most unstable eigenstate for a free-slip cell with a *conducting* sidewall is bounded below by the second unstable state of a cell with an *insulating* sidewall, a result that can be seen by the same reasoning used in proving Theorem 2.9. But it is easy to verify that the second unstable curve λ_2 in the $\lambda - L$ plot is monotonic between the two anchored states that are intersections of curves corresponding to $k_{m,j}, k_{m,j+1}$ and $k_{m,j}, k_{m,j+2}$, respectively. By the asymptotic formula $k_{m,j} \approx j\pi + \frac{\pi}{2}(m + \frac{1}{2})$ [18] and Eqn. (21) we conclude that $\lambda_2 = \mathcal{O}(L^{-2})$ for large L. Thus, the effect of perturbation on the sidewall thermal property is

always of order $\mathcal{O}(L^{-2})$. Translating this result in terms of R_C, we immediately have $R_C - R_{C0} = \mathcal{O}(L^{-2})$. Similar analysis shows perturbing the sidewall viscous boundary condition for the m=0 modes has the same effect. However, it is to be noted that simultaneous perturbation by α and β immediately destroys the anchored states. Also, we don't have any control on $m \neq 0$ modes when we vary α. This apparent difficulty can be easily handled once we realize *there are states that behave virtually like anchored states under any perturbations*, an interesting assertion that will be made precise below, using a rigid-rigid cell as demonstration.

When the two horizontal plates are rigid we have to use Eqn. (22) as the unperturbed system and tune α and β of the sidewall to study their effects. In contrast to the previous case, we don't have any anchored states this time because j, the quantum number that characterizes the number of radial rolls, is coupled to the z-dependence of the eigenstates, thus preventing us from constructing a linearly superposed state out of the two intersecting solutions to satisfy $\theta = 0$ or $\vec{u} = 0$ at $r = L$, as the case may be. However, we do have states that are practically anchored for all positive α and β! Let's consider states that have the same number of vertical rolls. (In reality, only the states of one vertical rolls are of interest to us.) Fix R to be $R_{C\infty}$. Again, the intersecting solutions at $L = L_{int}$ correspond to those that have different j values. In particular, the most unstable intersections consist of two solutions whose $j's$ differ only by one. From the asymptotic expression[18] $J_m(k_{m,j}) \approx \sqrt{\frac{2}{\pi k_{m,j}}} \cos\left(k_{m,j} - \frac{\pi}{2}(m + \frac{1}{2})\right)$ we

see $|J_m(k_{m,j+1} + J_m(k_{m,j})| = \mathcal{O}(\frac{1}{j}) = \mathcal{O}(\frac{1}{L_{int}})$ because j/L_{int}=constant for large L_{int}. Thus, the intersecting solutions differ only by $\mathcal{O}(\frac{1}{L_{int}})$ *on the sidewall.* Eqn. (8) then tells us one of the perturbed eigenstates will have θ almost zero on the sidewall because it is almost proportional to $J_m(k_{m,j+1}) + J_m(k_{m,j})$. This state in turn must remain practically fixed during the process of perturbation by Eqns. (3) and (4). More specifically, its perturbation will be $\mathcal{O}(L^{-1})$ smaller than that experienced by other states or states of different L. I would like to emphasize that this argument is apparently very general and applies to simultaneous perturbation of α and β as well. For example, we can choose $\alpha \equiv \tan(\frac{\pi}{2}\frac{\beta}{\beta_0})$ and let $\beta \to \beta_0$. The final configuration then corresponds to a cell with a rigid sidewall whose thermal property is $\frac{\partial\theta}{\partial n} + \beta_0\theta = 0$.

We now examine the case when maximal perturbation is achieved, *i.e.*, $\alpha = \beta = +\infty$. Our argument plus the monotonicity Theorem 2 imply $\lambda = -\mathcal{O}(L^{-2})$ monotonically in L. What is more, we can easily see from smoothness that the difference between $\lambda(L)$ and $\lambda_{\text{int}}(L)$, the curve obtained by "analytically continuing" $\lambda_{\text{int}}(L_{\text{int}})$ in L_{int} for the intersecting eigenvalue λ_{int}, is of order $\mathcal{O}\ (L_{int}^{-3})$. ($\lambda_{\text{int}}$ is given by Eqn. (A.3) of Appendix A for a one-dimensional problem. The scalings for both cases are the same.)

Next we can reverse the direction of perturbations and start with this rigid and perfectly conducting case. Because the "unperturbed" curve $\lambda(L)$ is smooth, as opposed to our original perturbation from the free-slip and insulating case when

the most unstable mode has a kink at every intersection, we know the effect of the perturbation must always be of order $\mathcal{O}(L^{-3})$ because all the practically anchored states are perturbed by $\mathcal{O}(L^{-3})$ only. This is true for any perturbation of the type $\beta_1 \frac{\partial \theta}{\partial n} + \theta = 0$ and $\alpha_1 \frac{\partial \vec{u}_\parallel}{\partial n} + \vec{u}_\parallel = 0$, where α_1 and β_1 are nonnegative.

The implication of this argument is: if we turn on the perturbation from the free-slip and insulating case, say $\frac{\partial \theta}{\partial n} + \beta\theta = 0$ for some very small but fixed $\beta > 0$, then there must be a cross-over size L_{C-O} above which $\lambda(L) = \lambda_{\text{int}}(L) + \mathcal{O}(L^{-3})$ is valid. In other words, no matter how small the perturbation is, the structure of the "tail" of the unperturbed $\lambda(L)$ is immediately destroyed for all large enough L, and is replaced by a smooth curve that is practically independent of the perturbation strength. This curve deviates from $\lambda_{\text{int}}(L)$ only by $\mathcal{O}(L^{-3})$. (Of course, L_{C-O} will depend sensitively on the perturbation strength. The smaller the perturbation, the larger L_{C-O} becomes.)

All the previous predictions concerning the behavior of λ can be easily translated in terms of R_c. What is worth mentioning is that our argument is essentially one-dimensional and, thus, not surprisingly, bears all the features of the example we study in detail in Appendix A.

For a cell Ω of arbitrary geometry we can find two concentric cylindrical cells Ω_1 and Ω_2 such that $\Omega_1 \subset \Omega \subset \Omega_2$. Then Theorem 2 together with the above analysis for cylindrical cells imply similar L^{-2} scaling of $R_C - R_{C\infty}$ for Ω when the sidewall is rigid and perfectly conducting. If Ω doesn't possess any symmetry that

causes degeneracy in this most stable configuration, then the effect of boundary perturbation can only give rise to the $\mathcal{O}(L^{-3})$ effect, and our basic conclusion won't change. On the other hand, we can group solutions with specific symmetry to remove annoying degeneracy if the cell possesses particular symmetries itself. Therefore, it is expected that the L^{-2} scaling and the immediate destruction of the large L "tail" of $\lambda(L)$ curve under perturbation from the analytically solvable cell with free-slip and insulating sidewalls are generally true.

At this point it is worth mentioning that if we are interested in the behavior of R_C alone, then we can take the more direct approach of performing entirely analogous perturbation calculations on R_C and combining the results with Variational Principle II to derive all the conclusions I described above that were obtained indirectly *via* studying the growth rate λ. The advantage one gains is that we don't have to worry about the complication introduced by the vertical vorticity because it is identically zero, as is shown in Appendix B. But then the analogy with the reaction-diffusion models of developmental biology is less direct. As a final remark, we observe that the L^{-2} scaling I derived above and Eqn. (12) suggest that the temperature (and velocity as well, if we include α term in it to make it completely general; see the remark following Theorem 3) must drop to $\mathcal{O}(L^{-1})$ near the sidewall for general boundary conditions. Although I only derived Eqn. (12) for a rectangular cell, it clearly holds for cells of other shapes as long as the sidewalls don't get too rugged. This can be seen by perturbing the boundary of

a rectangular cell: one can derive formulas similar to Eqn. (11) to show that the perturbation to the eigenstates is always of order $\mathcal{O}(L^{-2})$ near the sidewall and can not alter our observation. It is interesting to note that the same conclusion for a one-dimensional problem can be predicted *via* a two-scale amplitude equation approach.[29] My analysis, therefore, not only gives an independent verification to that approach, but also asserts this is a general phenomenon expected for three-dimensional convection in a cell of arbitrary geometry.

§3.2 Surrogate Versus Real System:

The effects of the sidewall on the marginally stable state can, in principle, be described by a mathematically equivalent boundary condition imposed on the convection cell. This is possible because at criticality the sidewall temperature θ_w satisfies the Laplace equation and, thus, admits elimination of θ_w in favor of fluid temperature θ on $\partial\Omega$. In the following, we shall denote the outer surface of the sidewall by S_2 and the inner surface by S. Let $g_1(\vec{r},\vec{r}')$ be the Green's function for $-\nabla^2$ inside the wall with vanishing $\frac{\partial g_1}{\partial n'}$ on S_2 and g_1 on $\partial\Omega_w\backslash S_2$. Then $\theta_w = \int_S \frac{\partial g_1}{\partial n'}\theta'$, where $\vec{n}$ is the *outward* normal to the cell and primed quantities are dummy variables in differentiation or integration. This allows us to rewrite the jump condition, Eqn. (1.12), in terms of fluid temperature θ on S alone when θ_w is substituted by the expression derived above. We can also use another Green's function, g_2, which satisfies the same boundary conditions as g_1 except $\frac{\partial g_2}{\partial n'}$=0 on

S to yield $\theta_w = -\kappa_w{}^{-1} \int_S g_2 \frac{\partial \theta'}{\partial n'}$. If we are interested in the small κ_w regime, as is the case if we are perturbing about a perfectly insulating sidewall, then it is more convenient to use the equivalent boundary condition that incorporates g_1. Analogously, a boundary condition that involves g_2 is appropriate for large κ_w regime. However, this approach is only useful in analysis because the equivalent boundary condition for θ is an integral equation defined on S.

The situation improves if the sidewall is very thin. Note that for a thin wall with thickness $\tau \ll 1$ and radius of curvature of the interface S we can approximate the temperature inside the wall by a quadratic in the (outward) radial coordinate ξ that is zero on S by definition:

$$\theta_w = \frac{-\xi^2 + 2\xi\tau}{2} \nabla_S^2 \theta + \theta \ , \tag{25}$$

where θ is the fluid temperature at $\xi = 0$ and ∇_S^2 is the two-dimensional Laplacian on S. Eqn. (1.12) then becomes

$$\frac{\partial \theta}{\partial n} = \kappa_w \tau \nabla_S^2 \theta \ . \tag{26}$$

When ∇_S^2 can be replaced by a negative number, as is the case if one considers a particular Fourier mode, then the surrogate boundary condition $\frac{\partial \theta}{\partial n} + \beta\theta = 0$ is recovered. (Notice that the effective thermal conductivity β in this case is indeed proportional to the true sidewall conductivity κ_w.)

The previous argument already suggests to us that the surrogate boundary condition does capture the underlying physics involving a real sidewall. In fact, we

can even derive a mathematically rigorous statement to quantify the vague idea of "capturing the underlying physics!" Let Ψ be the ground state for a cell with a real sidewall, then

$$\begin{aligned} \frac{\int_{\Omega_w} |\nabla\theta_w|^2}{\int_S \theta^2} &= \left(\frac{\int_{\Omega_w} |\nabla\theta_w|^2}{\int_{\Omega_w} \theta_w^2}\right)\left(\frac{\int_S \theta_w^2}{\int_{\Omega_w} \theta_w^2}\right)^{-1} \\ &\geq \frac{\zeta}{c_1\sqrt{\zeta}+c_2} \geq c \end{aligned} \tag{27}$$

for some constants c_1, c_2 and c, where ζ stands for the expression inside the first $(\cdots)$ which is $\geq \pi^{2*}$, and the boundary condition $\theta = \theta_w$ and the inequality announced in Lemma 2.1 bounding the second $(\cdots)$ by $\sqrt{\zeta}$ are exploited. If we define $\beta \equiv cr\kappa_w$ for a given κ_w and denote the restriction of Ψ on Ω by ψ, then

$$R_C^{SBC\,-1/2} \geq J^{SBC}[\psi] \geq J[\Psi] = R_C{}^{-1/2} \ , \tag{28}$$

i.e., the critical Rayleigh number for the real system is bounded below by that for a surrogate system with $\beta = cr\kappa_w$. Incidentally, we note that this immediately implies $R_C - R_{C\infty} = \mathcal{O}(L^{-2})$ if the thickness of the sidewall remains about the same when one increases L, because for the surrogate system we have proved this is true in the previous section.

Next, I argue that we can also bound R_C from above by R_C^{SBC} of another surrogate system with $\beta = c'r\kappa_w$ for some constant c'. I shall show that actually this is true for a cell with an infinitely extended sidewall. Then the statement is certainly true for a cell with a finite sidewall because I showed in Theorem 2.4 that

* See Eqn. (B.2) of Appendix B.

its R_C is even smaller. Let ψ be the ground state of the surrogate cell. Define a coordinate system $\xi - \eta$ in the wall region such that ξ is the arc length of the "radial coordinate" that is orthogonal to S and vanishes on S, whereas η is the coordinate on the two dimensional surface S' defined by ξ=constant. I will assume the coordinates are chosen so that the angle between the ξ curve and the surface normal to S' is bounded away from $\pi/2$. Construct a trial function Ψ for the real system with a laterally infinite sidewall by extending the definition of ψ into the wall region so that

$$\begin{aligned}\theta_w &\equiv \left(\theta + \frac{1}{r\kappa_w}\frac{\partial\theta}{\partial n} f_1\right) f_2 \\ &= \theta\left(1 - \frac{\beta}{r\kappa_w} f_1\right) f_2 \equiv \theta(1-\zeta f_1) f_2 \\ &\equiv \theta h f_2 \ ,\end{aligned}$$

where f_2 is a function of ξ that satisfies $f_2'(0) = 0$, $f_2(0) = 1$ and decays sufficiently fast to zero as ξ tends to ∞, while $f_1 \equiv \xi$ except when ξ is greater than some prescribed number δ, in which case we define $f_1 \equiv \delta$. Also, θ is the fluid temperature on S whose definition can be trivially extended into the whole wall region by $\theta(\xi,\eta) \equiv \theta(\eta)\big|_S$. Then

$$\begin{aligned}&\int_{\Omega_w} |\nabla\theta_w|^2 = \int_{\Omega_w} |hf_2\nabla\theta + \theta f_2\nabla h + \theta h\nabla f_2|^2 \\ &\le h_M^2 \int_{\Omega_w} |\nabla\theta|^2 f_2^2 + \zeta^2 \int_{\xi<\delta} \theta^2 f_2^2 + h_M^2 \int_{\Omega_w} \theta^2 |\nabla f_2|^2 \\ &\quad + 2\zeta h_M \int_{\xi<\delta} |\theta\nabla\theta| f_2^2 + 2h_M^2 \int_{\Omega_w} |\theta\nabla\theta| \cdot |f_2\nabla f_2| + 2\zeta h_M \int_{\xi<\delta} \theta^2 |f_2\nabla f_2| \\ &\le a\left(h_M^2 \int_S |\nabla_S\theta|^2 + (h_M+\delta_1\zeta)^2 \int_S \theta^2 + 2(\delta_1\zeta + h_M)h_M \sqrt{\int_S \theta^2 \int_S |\nabla_S\theta|^2}\right) , \quad (29)\end{aligned}$$

where h_M is the maximum of h, and a is some constant depending on the geometry of the cell and the coordinates we choose. In the above, δ_1 is a number that is proportional to $\sqrt{\delta}$ when δ is very small. Also, ∇_S is the gradient operator on the interface S. But we observe that for the ground state it is possible to find a constant b such that

$$\int_S |\nabla_S \theta|^2 \leq b^2 \int_S \theta^2 \tag{30}$$

for all β. First of all, this statement is trivially true if it so happens that θ is identically zero on S for all β. So we may consider the case when θ is identically zero on S only at some isolated points β_0 of $\beta \in [0, \infty)$. (The case $\beta_0 = \infty$ *is* included in this argument.) Near each of these points we can expand θ in a power series of a small parameter δ'. (We can take $\delta' \equiv \beta - \beta_0$ if β_0 is finite; the case $\beta_0 = \infty$ can be handled by taking $\delta' \equiv \beta^{-1}$.) Suppose $\theta = \theta_n \delta'^n + \cdots$ for some leading power n such that θ_n is not identically zero on S, then clearly Eqn. (30) is satisfied for some b. Also, for β outside the neighborhood centered at β_0 we know the left hand side of Eqn. (30) must be bounded from above because the eigenfunction is twice differentiable, while the right hand side is bounded away from zero by construction. And so a constant b certainly can be found to satisfy Eqn. (30). Therefore, Eqn. (29) can be further reduced to

$$\int_{\Omega_w} |\nabla \theta_w|^2 \leq a(bh_M + h_M + \delta_1 \zeta)^2 \int_S \theta^2 \ . \tag{31}$$

But one easily verifies

$$c' \equiv \frac{a^{-1} - 2(b+1)\delta_1 - \sqrt{(a^{-1} - 2(b+1)\delta_1)^2 - 4(b+1)^2\delta_1^2}}{2\delta_1^2}$$

is a positive solution to the following equation for ζ if δ is small enough:

$$a(bh_M + h_M + \delta_1\zeta)^2 \;=\; \Big[a(b+1+\delta_1\zeta)^2 =\Big]\;\zeta\;.$$

Choose the β for the surrogate system to be $c'r\kappa_w$ then the previous reasoning immediately implies

$$r\kappa_w \int_{\Omega_w} |\nabla\theta_w|^2 \leq \beta \int_S \theta^2\;,$$

which in turn tells us

$$R_C^{SBC^{-1/2}} \equiv J^{SBC}[\psi] \leq J[\Psi] \leq R_C{}^{-1/2}\;, \tag{32}$$

by virtue of the variational principles for both systems.

To summarize, I have shown that, as far as marginal stability is concerned, under suitable conditions the true system with sidewall conductivity κ_w is sandwiched between two surrogate systems whose effective sidewall conductivities are proportional to κ_w. This means that using the simpler surrogate boundary condition to investigate the convective instability still retains the correct underlying physics furnished by the sidewall.

Chapter 4: Convective Rolls Near the Sidewalls

It is sometimes observed that in the visualization of stationary convection patterns using shadowgraphic technique, the convective rolls tend to align themselves normal to the sidewalls.[14,15] However, the interpretation of this observation is not immediately clear because the light rays projected on the screen above the cell to form observed patterns necessarily have to go through a series of focusing and defocusing processes caused by density variation upon passage through the entire fluid layer. A sensible definition of a roll that is theoretically simple and experimentally justifiable doesn't seem to exist at this moment. With this precaution in mind, and in view of the fact that intuitively we know the density variations on the two sides of a convective roll, whatever its definition may be, must be opposite in signs to account for the rising and lowering fluid motion about the roll axis, I have decided to take a simplistic approach of identifying the nodal surfaces of the density variation with typical convective rolls. This necessarily makes this chapter somewhat controversial and more on the speculative side, although I believe it still offers some insight to what people observe in the lab. By the assumed linearity between temperature and density, this means the nodal surfaces of θ will represent convective rolls in this convention.

For a time-independent solution, Eqn. (1.9) reduces to $\nabla^2\theta = 0$ on the boundary, *provided it is rigid*, a condition we shall assume throughout this chapter. For the given nodal surface OABC of θ in Fig. 4.1 we choose a local Cartesian

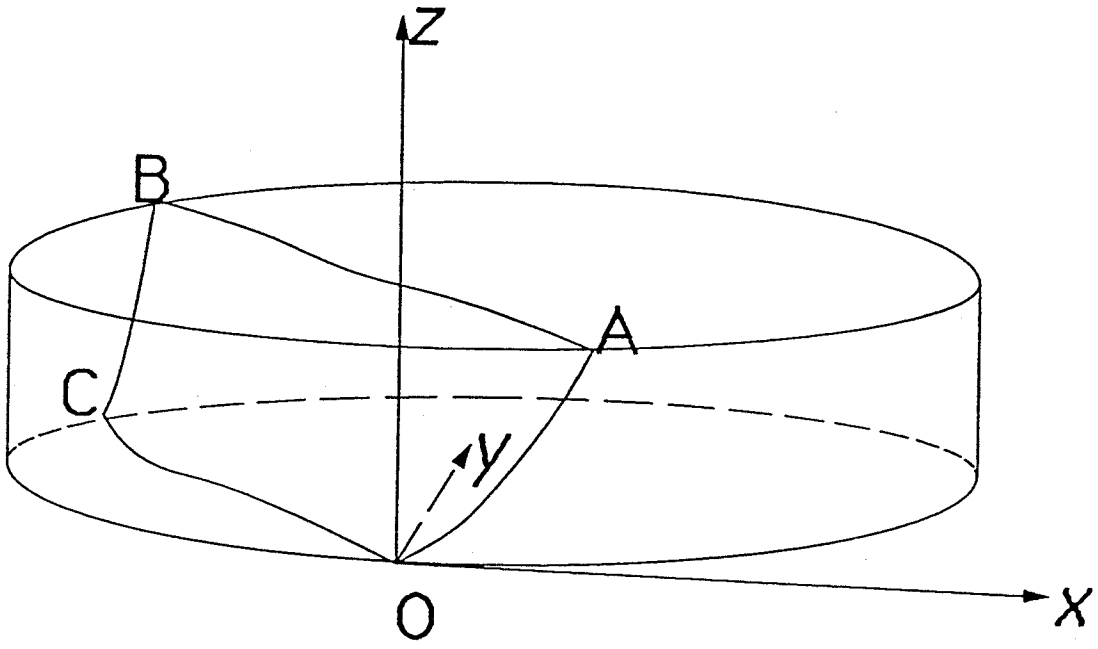

Figure 4.1: Local Cartesian coordinates x-y-z are chosen such that the origin O is at the intersection of temperature nodal surface OABC and the lower edge of the convection cell, and the x-axis is tangent to the sidewall.

coordinate such that the origin O is on the lower edge of the container and x is parallel to the sidewall. Because $\theta = 0$ at $z = 0$, we can expand θ in powers of z and write

$$\theta = fz + gz^3 + \mathcal{O}(z^4) \,, \tag{1}$$

where f and g are functions of x and y, and we have used the fact $\nabla^2\theta = 0$ at z=0 to kill the $\mathcal{O}(z^2)$ term. Therefore, we see that to the lowest order the nodal surfaces of θ are given by $z = 0$ (the bottom plate) and $f(x, y) = 0$. Notice the latter implies OABC is orthogonal to the bottom plate. Similarly it must be orthogonal to the

top plate.

Next, we investigate the behavior of OABC near the point O. Expanding $f \equiv ax + by$+(higher order terms) and imposing the thermal boundary condition $\frac{\partial \theta}{\partial n} + \beta\theta\big|_{y=0} = 0$, one obtains $b = 0$. Thus, to the lowest order $\theta = axz$ near the origin. The case $a \neq 0$ implies OABC is also orthogonal to the sidewall near point O. Parallelism of nodal surfaces to the sidewall corresponds to a nongeneric case in our analysis.

It is clear that the nodal surfaces still behave the same if the system is evolving according to linear stability analysis. The argument apparently is also valid for *binary* fluid convection when the Dufour effect, which describes the concentration-gradient induced heat current, can be neglected, because then the thermal equation is the same as Eqn. (1.9).

The implication of the previous argument seems to be: if the nodal surfaces of θ more or less correspond to the convective rolls one observes in experiments, then the orthogonality of rolls to the sidewalls is a simple consequence of the imposed realistic boundary conditions which render the governing equations linear close to the boundary. However, I must admit that this treatment is limited because it can not explain rigorously why visualization experiments using Doppler anemometry or other visualization techniques still observe rolls ending perpendicular to the sidewalls,[16–18] though intuitively we know the correlation between u_z and θ should imply the orthogonality of the former if the latter is perpendicular to the sidewalls.

Also, one would like to resolve the apparent difference between my conclusion and calculations made by Cross[30] using the amplitude equation approach that assert the possibility of having rolls approach the sidewall at an arbitrary angle. It seems likely that his calling upon the excitation of conjugate rolls near the sidewall to satisfy the boundary conditions has the effects of generating a cellular pattern and reorienting the temperature nodal surfaces so that they will tend to end perpendicular to the sidewall. In other words, the two approaches are designed to treat phenomena of different length scales. However, further work must be done before this question can be completely answered.

Chapter 5: Conclusion

I have shown that the linear analysis of the onset instability of Rayleigh-Bénard convection can be facilitated by a combination of a variational formalism and perturbation theory. In particular, the sidewall thermal conductivity and the wall thickness affect the stability in a monotonic way. I also made a comparison of this system with standard pattern forming models of developmental biology, remarked on how the boundary conditions might affect the argument, and pointed out the similarity as well as difference between the two systems. I argued that the difference of the critical Rayleigh number and its infinite cell limit scales as the inverse square of the system size for almost all boundary conditions by studying a system with a mathematically simpler boundary condition, which is a common practice in this field, and then showed that this artificially constructed boundary condition does capture the correct physics because, in a mathematically well-defined sense, the true system behaves halfway in between two such model systems.

Although it appears that I have relied very heavily on the variational formulation in my argument so that it is not clear how this work can be generalized to other more complex systems, I would like to point out that in the more difficult problems one probably can start with perturbation theory right from the beginning, and try to do a path-following technique, as was also described in this work. The results one obtains are then still global in the parameter range. As a matter of fact, a majority of the results I described in this work were first conceived and

discovered by a purely perturbative approach. The variational formulation of the problem actually came at a much later stage in my investigation of the convective stability problem.

It is true that some of the predictions concerning the monotonic dependence of the stability on the control parameters of the system are hardly surprising because one's intuition clearly indicates so, yet we should notice this intuition actually breaks down for a rotating convection cell, as is shown both in numerical calculations and experiments.[31,32] Currently, there is no good theoretical understanding of why this should be so, and I would like to study this problem as the next step of extending my work in this direction.

Clearly lacking in the present work is the nonlinear aspect of the convection problem. This in no way reflects the current trend of research since most workers actually have been investigating it by different approaches with success. Indeed, the nonlinear dynamics and pattern formation in binary fluid convection have offered us a rich zoo of interesting phenomena that the system is bound to teach us much more in the future. The binary fluid convection, therefore, is another problem I would like to explore.

Another problem that has practical application in thin film drying is the surface tension driven convection originally observed by Bénard. The pattern formation problem associated with this system doesn't seem to have drawn as much attention as its buoyancy driven cousin, although in recent years more work has

been done.[33–37] Unlike the previously mentioned problems which I myself actually have been studying for some time, this problem is only an acquaintance to me at this moment. I think an understanding of Rayleigh-Bénard convection can not be called complete unless the earliest reported phenomenon that originated all the beautiful work done by many of the finest experimentalists and theorists in the field for almost a century is properly studied and understood. With this problem in mind I hereby conclude this report of the first step of my study of the convection problem.

Appendix A

In this appendix I present the study of a one-dimensional surrogate system in detail to illustrate the ideas proposed in Chapter 3. Sophistication to the model will increase as we proceed.

We start with a cell Ω of dimension L that is completely free-slip and has perfectly insulated sides at $x = \pm\frac{L}{2}$. The two horizontal plates are located at $z = \pm\frac{1}{2}$. The solution for this problem is

$$\lambda = \frac{1+\sigma \pm \sqrt{(1+\sigma)^2 - 4\sigma(1-\frac{R}{\mu^2}(1-\frac{\mu_z}{\mu}))}}{2} \cdot \mu \ , \qquad (A.1)$$

$$\begin{aligned} \theta &= \sin n\pi(z+\frac{1}{2})\cos j\pi(\frac{x}{L}+\frac{1}{2}) \ , \\ u_z &\propto -\frac{j}{nL}\sin n\pi(z+\frac{1}{2})\cos j\pi(\frac{x}{L}+\frac{1}{2}) \ , \\ u_x &\propto \cos n\pi(z+\frac{1}{2})\sin j\pi(\frac{x}{L}+\frac{1}{2}) \ , \\ p &\propto \cos n\pi(z+\frac{1}{2})\cos j\pi(\frac{x}{L}+\frac{1}{2}) \ , \end{aligned} \qquad (A.2)$$

where $\mu = -((n\pi)^2 + (\frac{j\pi}{L})^2)$ and $\mu_z = -(n\pi)^2$ for integers n and j. We see from Eqn. (A.1) that it is possible to have $\frac{\partial\lambda}{\partial R} < 0$, although the most unstable state apparently satisfies $\frac{\partial\lambda}{\partial R} > 0$.

For purpose of illustration, we will fix n=1 and $R = R_{c0} \equiv \frac{27}{4}\pi^4$. The resulting λ vs. L curves with different j's are shown in Fig. A.1.

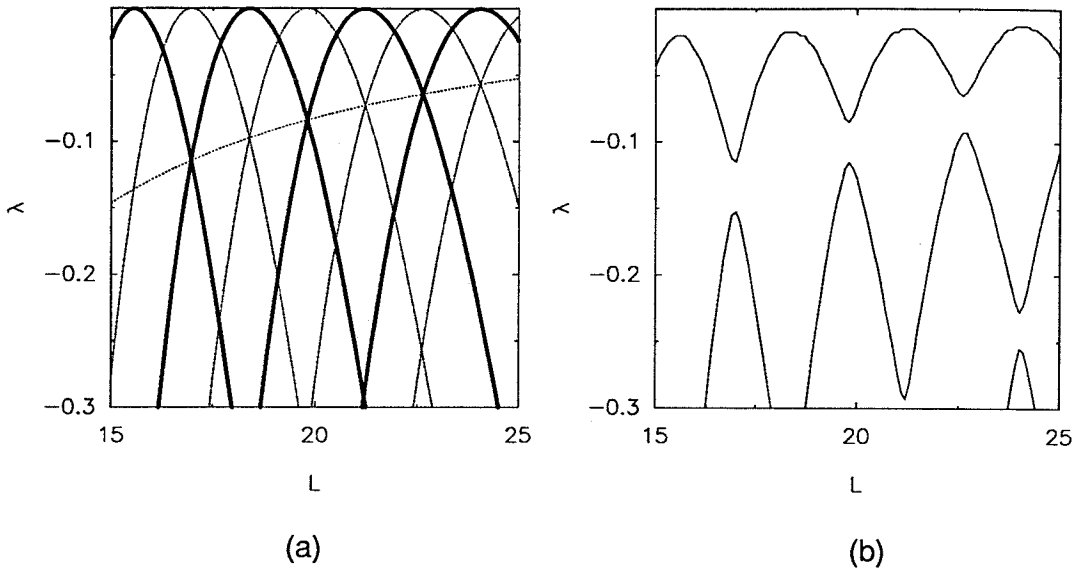

Figure A.1: (a) Growth rates λ vs. size L for a free-slip insulated two-dimensional cell are shown in dark or light, according to whether their symmetry under x -> -x is even or odd, when $R=R_{C0}$. The monotonic curve, given by Eqn. (A.3), connects intersections of curves j and j+2 (j=integer) that have the same symmetry. Biological pattern formation models show the same features. (b) Perturbing the dark curves by adjusting the sidewall property, in general, removes the degeneracies in (a) to form many wavy curves.

For any given j, λ vanishes when $L = \sqrt{2}j$. The intersection of curves j and $j+2$ which have the same symmetry under $x \to -x$ can be easily computed from Eqn. (A.1), and is given by

$$\lambda_{int} = -\frac{4\pi^2\sigma}{1+\sigma}\frac{1}{L_{int}^2} \qquad (A.3)$$

for large L_{int}, the size of the cell when degeneracy occurs. This curve is shown dotted in Fig. A.1. The size difference between two intersections ($j\&j+2$ and

$j+2\&j+4)$ is $\sqrt{2}$.

Also, notice in each degenerate two-dimensional subspace spanned by ψ_j and ψ_{j+2} we can find a vector $\psi \equiv \psi_j - \psi_{j+2}$ such that the associated $\theta \equiv \theta_j - \theta_{j+2} \propto (\cos j\pi(\frac{x}{L}+\frac{1}{2}) - \cos(j+2)\pi(\frac{x}{L}+\frac{1}{2}))$ vanishes identically at $x = \pm\frac{L}{2}$. Hence, $\theta = \frac{\partial\theta}{\partial n} = 0$, and the solution satisfies $\frac{\partial\theta}{\partial n}+\beta\theta = 0$ on $\partial\Omega$ for any β, *i.e.*, perturbation of β has no effect on ψ at all! These "anchored" solutions are clearly manifested in Fig. A.2(c) when translated in terms of R_c vs. L plot. Similarly, one can find anchored solutions when the viscous boundary condition is changed, though they will be different from the ones constructed above. The critical Rayleigh number at $L = L_{int}$ can also be calculated to give

$$R_c \approx R_{c0} + 18\frac{\pi^4}{L^2} \ . \qquad (A.4)$$

Next, we consider boundary perturbation of form $\frac{\partial\theta}{\partial n} + \beta\theta = 0$. To be specific, we'll consider θ that is odd in x. (Even solutions can be obtained by the replacement rule $k_j l \to k_j l + \frac{\pi}{2}$.) The problem is reduced to the following determinantal equation

$$\begin{vmatrix} \beta\sin k_1 l + k_1\cos k_1 l & \beta\sin k_2 l + k_2\cos k_2 l & \beta\sin k_3 l + k_3\cos k_3 l \\ (\lambda+\pi^2+k_1^2)k_1\cos k_1 l & (\lambda+\pi^2+k_2^2)k_2\cos k_2 l & (\lambda+\pi^2+k_3^2)k_3\cos k_3 l \\ \frac{(\lambda+\pi^2+k_1^2)}{k_1}\cos k_1 l & \frac{(\lambda+\pi^2+k_2^2)}{k_2}\cos k_2 l & \frac{(\lambda+\pi^2+k_3^2)}{k_3}\cos k_3 l \end{vmatrix} = 0 \ , \qquad (A.5)$$

where $l \equiv \frac{L}{2}$ and k_m^2 (m=1,2,3) are solutions to the dispersion relation

$$(\lambda+\pi^2+k_m^2)(\lambda+\sigma(\pi^2+k_m^2))(\pi^2+k_m^2) - R\sigma k_m^2 = 0 \ , \qquad (A.6)$$

and θ is some suitable linear combinations of $\sin\pi(z+\frac{1}{2})\sin k_j x$.

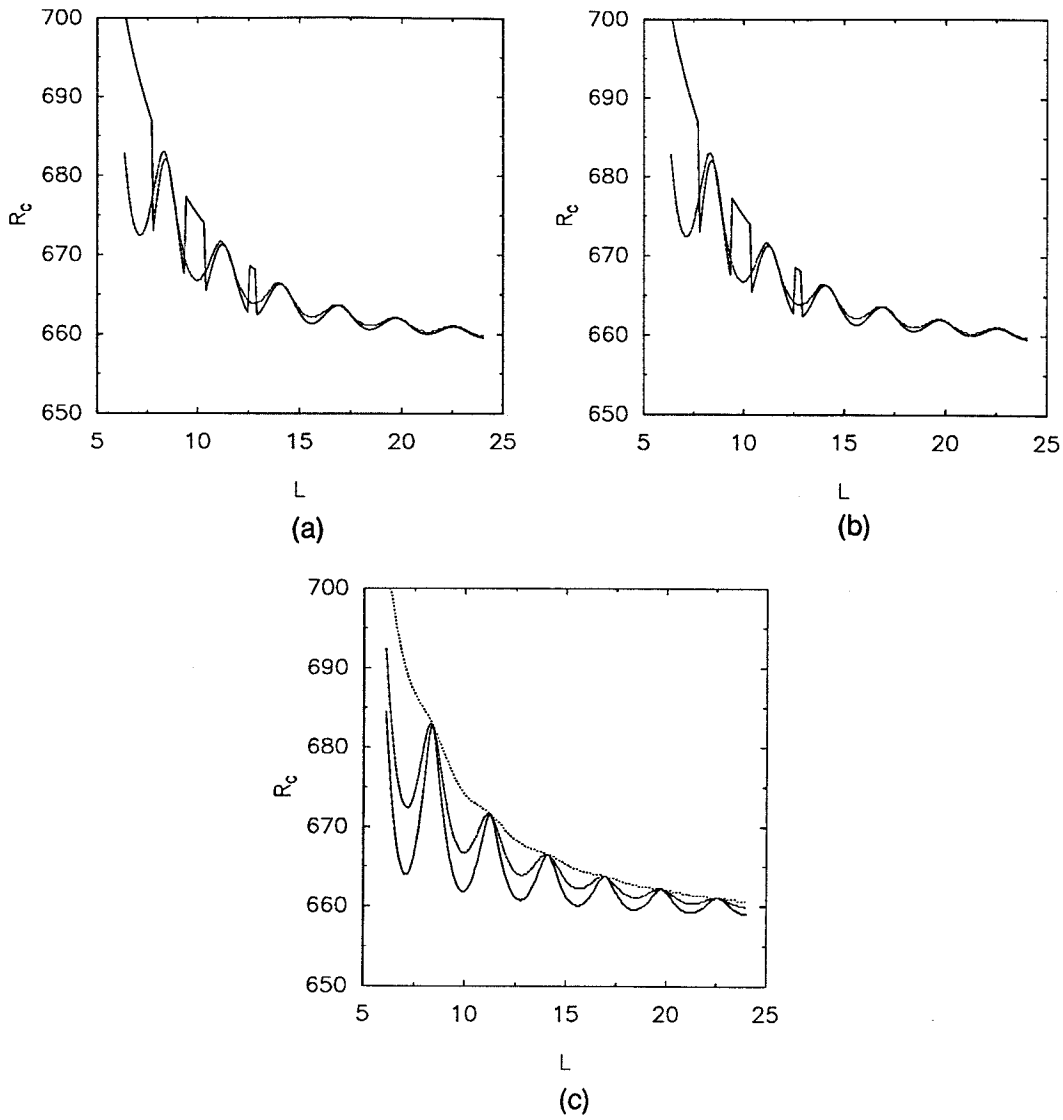

Figure A.2: Figures (a) and (b) show the prediction of Eqn. (A.9) and numerical results (smooth curves) for β=.3 and 1, respectively. ϕ_0 is set to zero whenever it is not defined for a given L. Solutions for β=.3, 1 and 50 are displayed in (c) to show the existence of "anchored states."

In the following, we'll consider the problem of determining R_c as a function of l. We can easily show that for a small deviation of $\Delta R \equiv R_c - R_{c0}$, k_m^2's are given by

$$k_{1,2} \approx \frac{\pi}{\sqrt{2}}(1 \pm \frac{\sqrt{\Delta R}}{3\pi^2} + \frac{7}{162}\frac{\Delta R}{\pi^4}) \,, \tag{A.7}$$

$$k_3 \approx 2i\pi(1 + \frac{2}{81}\frac{\Delta R}{\pi^4}) \,. \tag{A.8}$$

For $\Delta R > 0$, the lowest order solution to Eqn. (A.5) can be obtained by (1) dividing through the third column of the determinant by $\cos k_3 l$ and approximating $\tan k_3 l \approx i$ for large l, (2) allowing all the k_m's that don't appear as arguments of sinusoidal functions to assume their unperturbed values. The result is $\beta \sin(k_2 - k_1)l = 0$, or $\Delta R = 18\frac{\pi^4}{L^2}$, provided β is not too small. (We are extracting the leading order of Eqn. (A.5). Hence, the case β is very small must be handled separately. This is the first indication of the existence of a cross-over size L_{C-O} we discussed in Chapter 3.) Notice this lowest-order solution coincides with that given by (A.4)! As a matter of fact, this result can also be predicted using a two-scale amplitude equation.[29] The agreement between the two methods is not too surprising once we realize both approaches employ the same global phase drift $(k_2 - k_1)l$ to ensure that the correct boundary conditions are satisfied to the lowest order. To get the next order correction, we can rewrite Eqn. (A.5) as $\beta \sin(k_2 - k_1)l = f$ for some function f that also involves sinusoidal functions itself. Then one replaces the k_m's contained in f by their first order (correct to $\mathcal{O}(\sqrt{\Delta R})$) values so that

the equation is solved by $(k_2 - k_1)l = \pi - \phi_0 \equiv \pi\text{-}\sin^{-1}\frac{f}{\beta}$, or

$$\Delta R = \frac{18\pi^2(\pi - \phi_0)^2}{L^2} , \tag{A.9}$$

for some complicated function ϕ_0 that also involves L. Correct to order $\mathcal{O}(L^{-1})$ we find ϕ_0 is given by

$$\phi_0 = \sin^{-1}\left(-\left(\frac{\sqrt{2}}{9}\sin k_1 l + \left(\frac{4}{9} + \frac{2\pi}{\beta}\right)\cos k_1 l\right)\frac{\cos k_2 l}{l}\right) . \tag{A.10}$$

The point to be made is that for any fixed β, the oscillatory behavior as carried by ϕ_0 is always $\mathcal{O}(L^{-1})$ smaller than the "background" L^{-2} decay law given by Eqn. (A.4), thus confirming our claim in Chapter 3. Fig. A.2 shows the comparison between Eqn. (A.9) and numerical calculations.

For any given small positive β, the cross-over size can be estimated by requiring ϕ_0 to be well-defined for all $L > L_{C-O}$. Thus,

$$L_{C-O} \approx \frac{4\pi}{\beta} . \tag{A.11}$$

The R_c vs. L plot for solutions whose θ is even under $x \to -x$ looks very similar to that for odd θ when $\beta > 0$.

It is also easy to compute the solutions to Eqns. (A.5) and (A.6) when R is fixed while β is negatively very large. We find

$$\begin{gathered} k_1^2 \approx -\lambda, \quad k_2^2 \approx -\frac{\lambda}{\sigma}, \quad k_3^2 \approx -\pi^2, \\ i\beta + k_1 \approx 0. \end{gathered} \tag{A.12}$$

To lowest order the associated eigenvector is given by

$$\begin{aligned} u_x &\approx u_z \approx 0 \ , \\ \theta &\approx \sin \pi z \frac{\sin k_1 x}{\sin k_1 l} \ . \end{aligned} \tag{A.13}$$

This shows clearly that the run-away solution $\sqrt{\lambda} = -\beta$ develops a thermal boundary layer of thickness $-\beta^{-1}$ and strongly suppresses the velocity field.

It is apparent that all the previous results we have obtained through detailed analysis of a cell with free-slip sidewalls must similarly hold for a cell with rigid sidewalls because the methods we used work equally well for the latter. Instead of repeating the same analysis, we simply show, in Fig. A.3, the numerical calculations as further evidence supporting our claims.

As a final example, I present the numerical results of my study of a cell whose α on the two horizontal plates is also tunable. ($\alpha = \infty$ corresponds to a rigid-rigid cell.) Again, sidewall properties are tuned by (a different) α and β. The critical Rayleigh number is computed by maximizing $J^{SMC}[\psi]$ for ψ that is in a Hilbert subspace of finite dimension whose basis vectors θ and $\vec{u}$ are independently proportional to their corresponding variables given in Eqn. (A.2), with 15 modes of odd j and 5 modes of odd n.

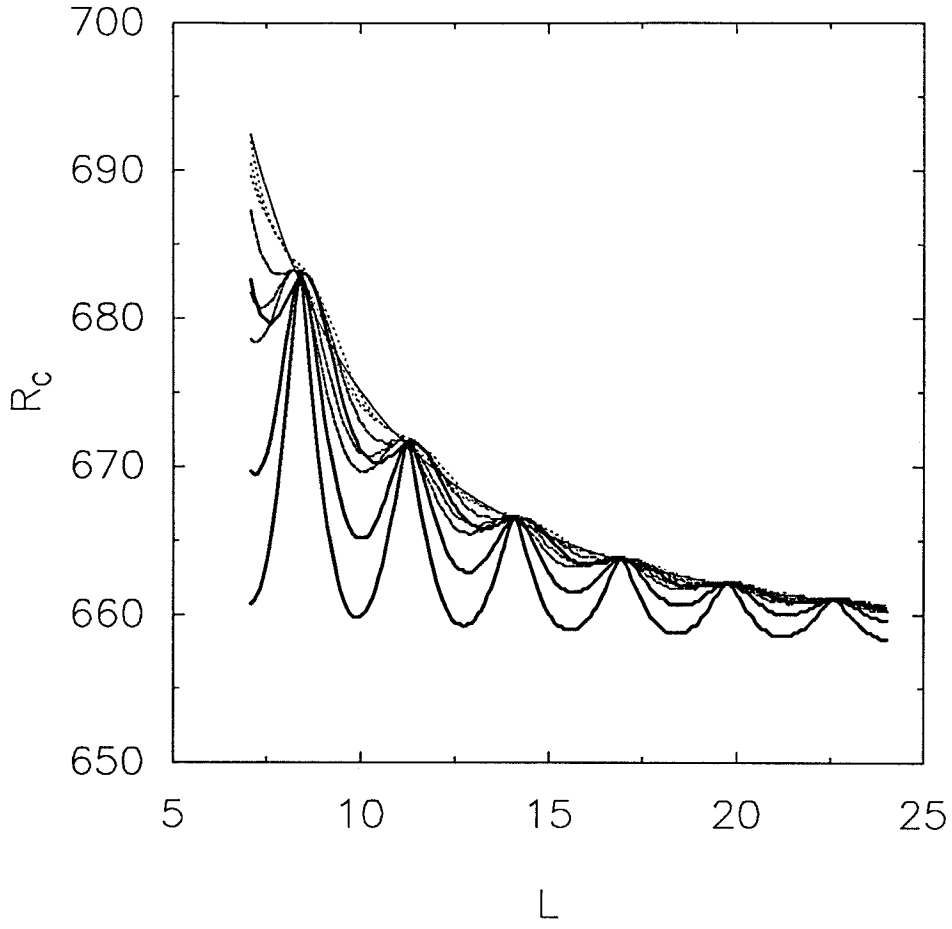

Figure A.3: Solutions for a free-slip cell with (α,β) taking all possible combinations from three values: .1, 2, and 50. The existence of the practically anchored states is obvious. The monotonically decreasing curve is calculated from Eqn. (A.4).

It is easy to show that this approach is actually just a variant of the mode expansion method one would use for solving a general linear problem in the sense that now we are simultaneously projecting both the governing equations and the boundary conditions onto the same conveniently chosen basis vectors. This particular projection scheme is favored over others because it is manifestly equivalent to

the variational principle, and the resulting generalized matrix eigenvalue problem is Hermitian. The results are shown in Fig. A.4. One is quickly convinced of the existence of the practically anchored states from this figure. Again, the basic features are not different from those for a free-slip cell.

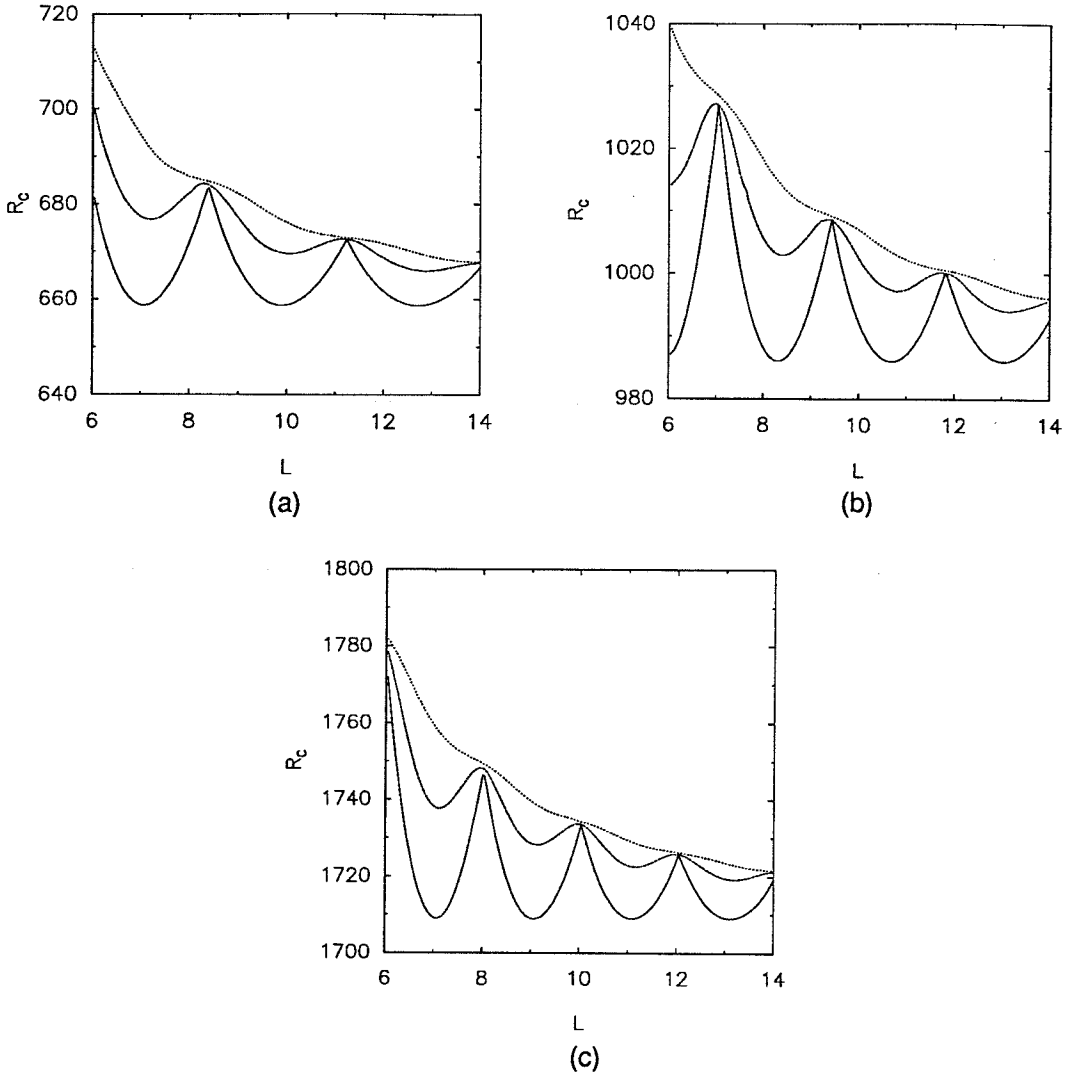

Figure A.4: Solutions for a cell with sidewall α and β taking three values: 0, 1, and 15. The two horizontal plates have an α= 0 (a), 4 (b), and 50 (c), respectively. The practically anchored states are clearly exhibited in the figures.

Appendix B

In this appendix, I will describe a simple sufficient condition for the method of separation of variables to hold for the convection cell. First, we need a simple estimate for a Rayleigh-Ritz ratio:

Lemma B.1

Let $f(z)$ be a trial function defined on [0,1]. Let λ_1 denote the ground state eigenvalue for $-\frac{d^2g}{dz^2} = \lambda g$, where g must satisfy $\pm\frac{dg}{dz} + \alpha g = 0$ at z=0,1 for some nonnegative constant α. Then for any f that is not identically zero we have

$$\begin{aligned} &\frac{\alpha(f^2(0) + f^2(1)) + \int_0^1 (\frac{df}{dz})^2 dz}{\int_0^1 f^2 dz} \\ &\geq \lambda_1 \geq \left(\frac{-\alpha + \sqrt{\alpha^2 + 8\pi^2\alpha}}{4\pi}\right)^2 . \end{aligned} \tag{B.1}$$

Proof:

The first inequality is the standard variational characterization for the eigenvalue λ_1. Therefore, we only need to prove the second inequality. Let $k \equiv \sqrt{\lambda_1} \in [0, \pi]$, then the boundary condition implies $\alpha = k \tan\frac{k}{2}$. By convexity of cosine function in the interval $[0, \frac{\pi}{2}]$, we know $\cos y \geq (1 - \frac{2y}{\pi})$ for all $y \in [0, \frac{\pi}{2}]$. Hence,

$$\int_0^{k/2} \frac{1}{(1 - \frac{2y}{\pi})^2} dy \geq \int_0^{k/2} \frac{1}{\cos^2 y} dy ,$$

which implies, upon evaluating the integrals, that

$$\frac{(\frac{k}{\pi})^2}{1 - \frac{k}{\pi}} \geq \frac{2}{\pi^2} k \tan\frac{k}{2} \equiv \frac{2}{\pi^2}\alpha .$$

Inverting this inequality immediately gives Eqn. (B.1).

Q.E.D.

Notice the above yields the following well-known assertion when applied to the case $\alpha = \infty$:

Corollary:

Any nonzero trial function f which satisfies the boundary condition $f(0) = f(1) = 0$ always satisfies

$$\frac{\int_0^1 \left(\frac{df}{dz}\right)^2 dz}{\int_0^1 f^2 dz} \geq \pi^2 \ . \tag{B.2}$$

More generally, the previous two assertions are still true if f is a function defined on a three-dimensional cell Ω, provided we substitute $\frac{df}{dz}$ by ∇f, $f^2(0) + f^2(1)$ by $\int_{\partial\Omega} f^2$, and $\int_0^1 dz$ by $\int_\Omega$.

Suppose the sidewall is perfectly insulating and we impose free slip boundary condition on it. Then we can expand both θ and u_z in an orthonormal basis φ_j's that are eigenfunctions of the two-dimensional Neumann Laplacian on the horizontal cross section: $-\nabla_h^2 \varphi_j = \mu_j \varphi_j$. Of course, the "Fourier coefficients" will then be functions of z. Now if we look at Eqn. (2.1) it is clear that in order to decouple all the φ_j modes (so that we do have separation of variables) we must be able to write the horizontal component $\vec{u}_h$ of the fluid velocity as linear combinations of $\nabla_h \varphi$. (The pressure p is automatically expandable in φ_j's.)

This apparently implies the vertical vorticity ω must vanish. Thus, we are led to investigate when we can expect ω to vanish identically.

Taking the curl of the Navier-Stokes equation and projecting it to the $\hat{e}_z$ direction we obtain

$$\lambda\omega = \sigma\nabla^2\omega \ . \tag{B.3}$$

Assume ω is not identically zero, then upon multiplying Eqn. (B.3) by ω and integrating over the fluid cell Ω we get

$$\lambda = -\sigma\frac{\int_{\partial\Omega\setminus S}\alpha\omega^2 + \int_\Omega \|\nabla\omega\|^2}{\int_\Omega \omega^2} \leq \sigma\lambda_1 \leq -\sigma\left(\frac{-\alpha+\sqrt{\alpha^2+8\pi^2\alpha}}{4\pi}\right)^2 \ . \tag{B.4}$$

In arriving at this result I have performed integration by parts, imposed the boundary conditions of Eqns. (1.14) and (1.15) on the two horizontal plates, and made use of Eqn. (B.1) that was just derived. Hence, ω must vanish identically, thus permitting separation of variables, provided the growth rate of interest lies above the bound set up by Eqn. (B.4). If we recall the derivation of the large cell scaling behavior of λ or R_C for positive α in Section 3.1, we immediately see that the argument presented there was well justified, because for all large enough size L the relevant growth rate λ considered there actually goes to zero, and therefore does lie above the bound given by Eqn. (B.4).

I would also like to point out that had we started studying R_C directly without invoking λ, as opposed to what was done in Section 3.1, then all the orthonormal eigenfunctions (under the second norm defined there) have zero vorticity, and sep-

aration of variables certainly is all right if the sidewall is free slip and perfectly insulating.

References:

1. H. Bénard, *Revue Gén. Sci. Pur. Appl. 11,* 1261 and 1309 (1900).
2. P. G. Drazin and W. H. Reid, *Hydrodynamic Stability,* p. 32, Cambridge Univ. Press, New York, 1982.
3. J. Thomson, *Proc. Phil. Soc. Glasgow. 13,* 464 (1882).
4. Lord Rayleigh, *Phil. Mag. (6) 32,* 529 (1916).
5. H. Jeffreys, *Proc. Roy. Soc. A 118,* 195 (1928).
6. A. R. Low, *Proc. Roy. Soc. A 125,* 180 (1929).
7. A. Pellew and R.V. Southwell, *Proc. Roy. Soc. (London) A 176,* 312 (1940).
8. V. S. Sorokin, *Prikl. Mat. Mekh. 17,* 39 (1953); V. S. Sorokin and I. V. Sushkin, *Soviet Phys. JETP 11,* 440 (1960).
9. E. N. Lorenz, *J. Atmos. Sci. 20,* 130 (1963).
10. L. A. Segel, *J. Fluid Mech. 30,* 625 (1967).
11. A. C. Newell and J.A. Whitehead, *J. Fluid Mech. 38,* 279 (1969).
12. M. J. Block, *Nature 178,* 650 (1956).
13. J. R. A. Pearson, *J. Fluid. Mech. 4,* 489 (1958).
14. V. Croquette, *Contemp. Phys. 30,* 113 (1989); V. Croquette, *Contemp. Phys. 30,* 153 (1989).
15. V. Croquette, M. Mory and F. Schosseler, *J. Physique 44,* 293 (1983).
16. J. P. Gollub and J. F. Steinman, *Phys. Rev. Lett. 47,* 505 (1981).
17. P. Bergé and M. Dubois, in *Systems Far from Equilibrium,* Springer-Verlag,

1980.

18. E. Somerscales and D. Dropkin, *Int. J. Heat Mass Trans. 9,* 1189 (1966).

19. D. E. Gray (ed.), *American Institute of Physics Handbook,* McGraw-Hill Book Company, Inc., 1957.

20. E. A. Spiegel and G. Veronis, *Astrophys. J. 131,* 442 (1960).

21. J. M. Mihaljan, *Astrophys. J. 136,* 1126 (1962).

22. O. D. Gray and A. Giorgini, *Int. J. Heat Mass Transfer 19,* 545 (1976).

23. S. Chandrasekhar, *Hydrodynamic and Hydromagnetic Stability,* pp. 27ff, Oxford Univ. Press, 1961.

24. R. Courant and D. Hilbert, *Methods of Mathematical Physics,* Vol. I, Chapter VI, Interscience Pub. Inc., 1966.

25. For an elementary treatment of the simpler Laplacian operator that actually can be generalized to our problem, see P. R. Garabedian, *Partial Differential Equations,* Chap. 10, John Wiley & Sons, Inc., 1964. For the treatments of the linearized Navier-Stokes equation, see O. A. Ladyzhenskaya, *The Mathematical Theory of Viscous Incompressible Flow,* Gordon and Breach Science Publishers, Inc. , 1963 and V. I. Yudovich, *The Linearization Method in Hydrodynamical Stability Theory,* American Mathematical Society, 1989.

26. M. P. do Carmo, *Differential Geometry of Curves and Surfaces,* p. 297, Prentice-Hall Inc., 1976.

27. A. Shapere and F. Wilczek (ed.), *Geometric Phases in Physics,* World Scien-

tific, 1989.

28. J. D. Murray, *Mathematical Biology,* Chapters 14 and 15, Springer-Verlag, 1989.

29. M. C. Cross, P. G. Daniels, P. C. Hohenberg and E. D. Siggia, *J. Fluid Mech. 127,* 155 (1983).

30. M. C. Cross, *Phys. Fluids 25,* 936 (1982).

31. F. Zhong, R. Ecke and V. Steinberg, preprint (1991).

32. J. C. Buell and I. Catton, *Phys. Fluids 26,* 892 (1983).

33. E. L. Koschmieder and S. A. Prahl, *J. Fluid Mech. 215,* 571 (1989).

34. A. Cloot and G. Lebon, *Phys. Fluids A 2,* 525 (1990).

35. G. Gouesbet, J. Maquet, C. Rozé, and R. Darrigo, *Phys. Fluids A 2,* 903 (1990).

36. M. J. Tan, S. G. Bankoff and S. H. Davis, *Phys. Fluids A 2,* 313 (1990).

37. J.P. Burelbach, S.G. Bankoff and S.H. Davis, *Phys. Fluids A 2,* 322 (1990).